RSC Advances

PAPER

View Article Online
View Journal | View Issue

Check for updates

Cite this: *RSC Adv.*, 2022, **12**, 32082

Effects of fluorine bonding and nonbonding interactions on ^{19}F chemical shifts†

Yang Lu, [a] Mingming Sun[c] and Ning Xi *[ab]

Received 21st October 2022
Accepted 25th October 2022

DOI: 10.1039/d2ra06660b

rsc.li/rsc-advances

^{19}F-NMR signals are sensitive to local electrostatic fields and are useful in probing protein structures and dynamics. Here, we used chemically identical *ortho*-F nuclei in *N*-phenyl γ-lactams to investigate the relationship between ^{19}F NMR chemical shifts and local environments. By varying the structures at the C5- and C7-substituents, we demonstrated that ^{19}F shifts and Hammett coefficients in Hammett plots follow typical relationships in bonding interactions, while manifesting reverse correlations in nonbonding contacts. Quantum mechanics calculations revealed that one of the *ortho*-F nuclei engages in n → π* orbital delocalization between F lone pair electrons (n) and a C=O/Ar=N antibonding orbital (π*), and the other *ortho*-F nucleus exhibits n ↔ σ orbital polarization between the n electrons and the C–H σ bonding orbital. As ^{19}F NMR spectroscopy find increasing use in molecular sensors and biological sciences, our findings are valuable for designing sensitive probes, elucidating molecular structures, and quantifying analytes.

1. Introduction

Fluorine is a particularly important element in the broader space of chemical biology. Many FDA approved drugs and commercial compounds such as pesticides and refrigerants are fluorinated.[1] There is a high degree of interaction between fluorine and biomolecules, which plays an important role in the functioning of fluorinated molecules.[2] Owing to the lack of naturally-occurring fluorinated organic molecules, fluorine is also a unique probe to investigate the structures and functions of biological molecules,[3] and a feasible sensor to detect analytes of biological, medicinal, and environmental importance.[4] Central to these studies is ^{19}F NMR spectroscopy, which allows users to readily visualize ^{19}F chemical shifts and splitting patterns depending on the fluorine local chemical environments.

The ^{19}F isotope is 100% naturally abundant and shows a large NMR chemical shift range (~300 ppm). The high resolution, coupled with high detection sensitivity and absence of background signals, affords well-resolved ^{19}F resonances. To date, ^{19}F NMR spectroscopy has been extensively applied in diverse biological, pharmaceutical, and material researches as evidenced by new reporter molecules and detection strategies.[3,4] Zhao and Swager,[5] as well as our own work,[6] showed that ^{19}F signals are sensitive to chiral environments even though the stereogenic centers are several carbons away from the fluorine. Recently, Prof. Huang and Zhao confirmed that substituents adjacent and distal to F are both important to the resolving ability of ^{19}F-labeled sensors.[7] In fact, the rich information obtained from ^{19}F NMR spectroscopy also allows us to monitor molecular interaction and dynamics. Related studies based on fluorinated ligands and/or fluorinated proteins have found their broad utilities in molecular recognition, protein/nucleic acid characterization,[3] and fragment-based drug discovery.[8] However, interpreting ^{19}F NMR data from biomolecular mixtures can be challenging and is often complicated by the lack of knowledge in ^{19}F chemical shift assignments, among others.

In order to better use of fluorinated molecules in biochemical applications, a comprehensive understanding of correlations between ^{19}F chemical shift and the environment/structure is essential. It is well-recognized that ^{19}F shielding is not only determined by magnetic anisotropies associated with the covalent bond system and with the circulation of π-electrons in aromatic rings, but also greatly influenced by van der Waals interactions, hydrogen bonding, and electric fields.[9] Non-covalent interactions such as multipolar contacts in C–F···C=O and C–F···C=N pairs,[10] hydrogen-bonding in C–F···H–N, C–F···H–O, and C–F···H–C pairs,[11] and interactions found in C–F···S[12a] and C–F···π pairs,[12b] have been reported. Sporadic data disclosed in literature suggest that C–F···H–X interactions shield ^{19}F signals.[13] Prof. Lectka confirmed that ^{19}F signals in "jousting" C–F···H–C interactions display remarkable downfield shifts, likely due to dominating repulsive forces between

[a]*Institute of Drug Discovery Technology, Ningbo University, Ningbo, Zhejiang 315211, P. R. China. E-mail: xining@nbu.edu.cn*

[b]*School of Medicine, Ningbo University, Ningbo, Zhejiang 315211, P. R. China*

[c]*Department of Chemistry, Nanchang University, 999 Xuefu Avenue, Nanchang, 330031, P. R. China*

† Electronic supplementary information (ESI) available. CCDC 1904410 and 1915197. For ESI and crystallographic data in CIF or other electronic format see DOI: https://doi.org/10.1039/d2ra06660b

Open Access Article. Published on 09 November 2022. Downloaded on 2/10/2026 6:58:20 PM. This article is licensed under a Creative Commons Attribution-NonCommercial 3.0 Unported Licence.

© 2022 The Author(s). Published by the Royal Society of Chemistry

Open Access Article. Published on 09 November 2022. Downloaded on 2/10/2026 6:58:20 PM.
This article is licensed under a Creative Commons Attribution-NonCommercial 3.0 Unported Licence.

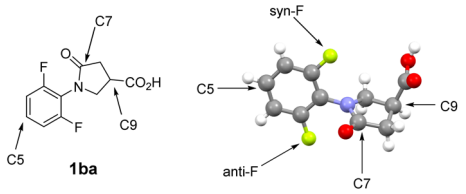

Fig. 1 Assignments of *syn*-F and *anti*-F nuclei on *N*-phenyl group. The atom numbers are assigned according to crystal structures.

C–F···H–C.[14] Yet, the effects of C=O/C=N groups on ^{19}F chemical shifts are not reported in the public domain, and a full understanding of relations between ^{19}F chemical shifts and chemical environments remains elusive.

We have employed a slow rotating (on ^{19}F NMR time scale), di-*ortho*-F substituted *N*-phenyl γ-lactam scaffold to study through-space contacts of F with remote functional groups such as stereogenic C9-amides and C9-esters, as shown in Fig. 1.[15] Compounds are generally used as enantiomeric mixtures, as the individual enantiomer behaves the same spectroscopically. Assuming γ-lactam ring as a flat ring, we define the *ortho*-F nucleus siting on the same side of C9-substituents as *syn*-F, and the other *ortho*-F as *anti*-F (atom number assigned according to crystal structures, *vide infra*). By varying the *p*-substituent on C9-phenylamide, we showed that downfield ^{19}F shifts δ_{down} display "reverse" a linear relationship with Hammett constants σ_{para} of the *p*-substituents. There are only small changes at the upfield ^{19}F shifts δ_{up} in various C9-amide derivatives. We therefore assigned the downfield ^{19}F signal to *syn*-F, and the upfield ^{19}F peak to *anti*-F.[16] In this report, we examined correlations of ^{19}F chemical shifts with different C7- and C5-groups in γ-lactam-derived structures. We also carried out quantum calculations to investigate fluorine through-space contacts with the adjacent functional groups. Effects of through-bond and through-space interactions on ^{19}F chemical shifts, as well as the through-space orbital delocalization are discussed.

2. Results and discussion

In di-*ortho*-F substituted *N*-phenyl γ-lactam derivatives, structural modifications of γ-lactam ring initiate unequal perturbations on *ortho*-F nuclei regarding to their through-space interactions, but afford the same through-bond effects on *syn*-F and *anti*-F. Thus, converting C7-amide to C7-thioamide or C7-amidine moiety on the γ-lactam ring alters chemical environments around *syn*-F and *anti*-F differently, as exemplified in thioamides **2a–f** and amidines **4a–q**. Installing a substituent at C5 on *N*-phenyl group, as in compounds **6a–w**, produces the same bonding and nonbonding effects on both *ortho*-F nuclei. Fig. 2 shows the chemical structures of compounds **1–6**, where structures of **1a–f**, **3a–e** and **5a–i** are used as references to the corresponding C9-esters/amides.

2.1. Synthetic schemes

Illustrative synthetic schemes for compounds **2–6** are provided in Fig. 3–5. Compounds **2a** and **2b** were converted from **1a** and

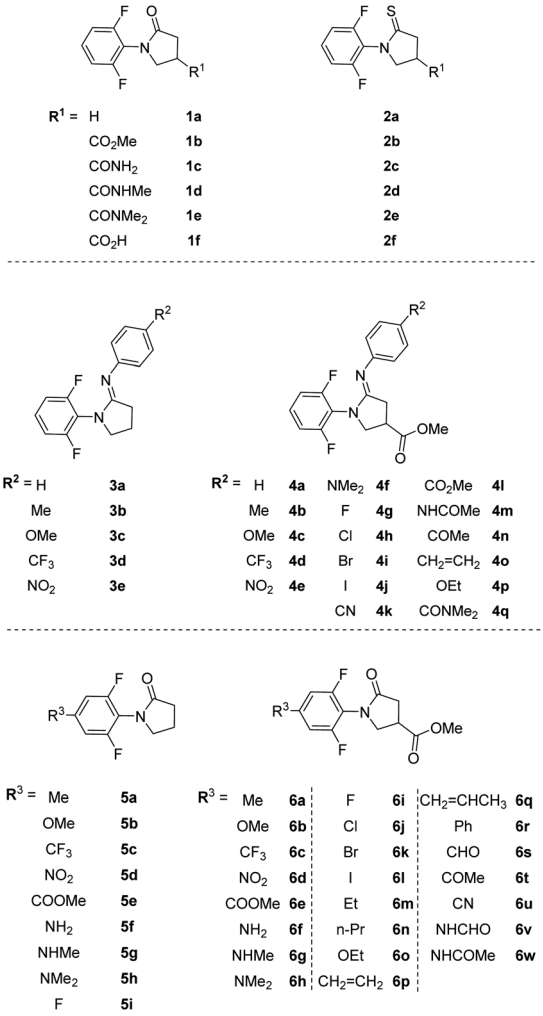

Fig. 2 Structures of compounds **1–6**.

1b, respectively, with Lawesson's reagent under mild conditions.[17] For C7-phenylamidine derivatives **3** and **4**, two synthetic routes were employed. The initial procedure requires the presence of $POCl_3$ in CH_2Cl_2 solution under refluxing conditions.[18] This one-pot reaction was used to generate compounds **3a–e** and **4a–e**. A more versatile and productive approach was later developed using thioamide **2b** as the starting material.[19] As shown in Fig. 3, thioamide **2b** was treated with mCPBA at 0 °C, followed by the addition of *para*-substituted phenylamines to give the desired amidines **4f–q**. This process is compatible with basic *para*-substituents such as dimethylamine (NMe_2) and generally provides better yields than the $POCl_3$ route.

C5-substituted *N*-phenyl γ-lactams **6a–e**, **6i–o** and **6u** were obtained through the synthetic routes as described previously, starting from appropriate 5-substituted anilines.[15] The syntheses of **5f** and **6f** were attained by reducing the NO_2 group in **5e** or **6e**. Reductive aminations of **5f** and **6f** with $NaBH_4$ resulted in a mixture of anilines, which was separated by a column chromatography to give **5g**/**5h** and **6g**/**6h**. Acylation of **6f** with different acylating agents (formal or acetic acid) afforded **6v** and **6w** in excellent yields, as illustrated in Fig. 4.

© 2022 The Author(s). Published by the Royal Society of Chemistry

Open Access Article. Published on 09 November 2022. Downloaded on 2/10/2026 6:58:20 PM.
This article is licensed under a Creative Commons Attribution-NonCommercial 3.0 Unported Licence.

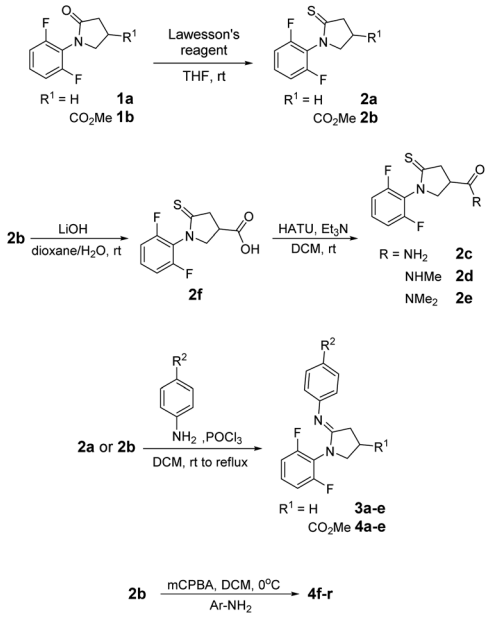

Fig. 3 Syntheses of compounds **2–4**.

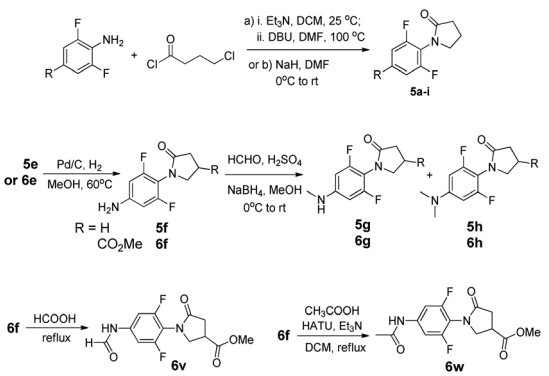

Fig. 4 Syntheses of compounds **5–6**.

Fig. 5 shows the syntheses of **6p–t** from 4-iodo **6l** through Pd-catalyzed coupling reactions. Stille coupling was used to obtain **6p** and **6q**,[20] while Suzuki–Miyaura coupling afforded **6r**. Formylation of aryl halides from **6l** using *t*-butyl isocyanide as a C1 source and formate salts as a hydride donor provided **6s**.[21] Similarly, vinylation of **6l** with a vinyl ether followed by hydrolysis furnished ketone **6t**.[22]

2.2. C7-substituent effects on *ortho*-^{19}F chemical shifts

We surveyed ^{19}F shift changes when the γ-lactam C=O group was converted into C=S and C=NPh groups. All ^{19}F NMR spectra were recorded in $CDCl_3$ solution at 25 °C. Compound concentrations were ~10 mg mL^{-1} and $CFCl_3$ was used as an internal standard. As shown in Tables 1 and 2, ^{19}F NMR signals become deshielded from −117.82 to −117.49 and −117.05 ppm, respectively, from compounds **1a** to **2a** and **3a**, likely due to their different electron-withdrawing abilities and polarizabilities. In chiral C9-ester series, thioamide **2b** and amidine **4a** display

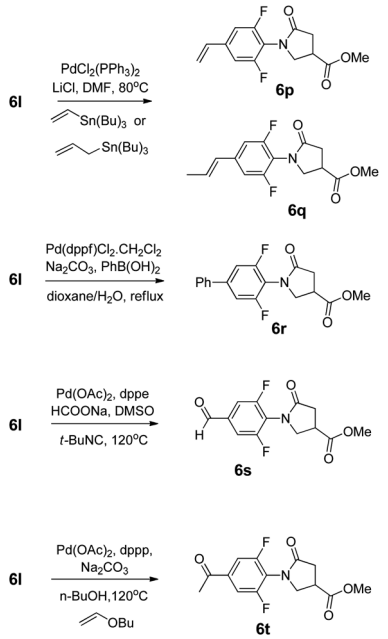

Fig. 5 Syntheses of compounds **6p–q** from **6f** and **6l**. [a] dppe: 1,2-bis(diphenylphosphino)ethane; dppp: 1,3-bis(di-phenylphosphino) propane; dppf: 1,1′-bis(diphnylphosphino)-ferrocene.

Table 1 ^{19}F NMR chemical shifts and calculated parameters for thioamide and amidine derivatives

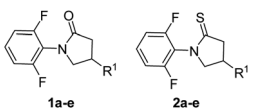

R^1		δ_{down}	δ_{up}	$\Delta\delta$		δ_{down}	δ_{up}	$\Delta\delta$
H	**1a**	−117.82	−117.82	0	**2a**	−117.49	−117.49	0
CO_2Me	**1b**	−117.14	−117.93	0.79	**2b**	−116.53	−117.69	1.16
$CONH_2$	**1c**	−116.81	−118.15	1.34	**2c**	−116.21	−117.94	1.73
CONHMe	**1d**	−116.66	−118.21	1.55	**2d**	−116.10	−118.07	1.98
$CONMe_2$	**1e**	−116.25	−118.23	1.98	**2e**	−115.59	−118.16	2.56

larger shift differences $\Delta\delta$ (1.16 and 1.09 ppm) between *syn*-F and *anti*-F signals than γ-lactam **1b** ($\Delta\delta = 0.79$ ppm). Therefore, the chemical environment differences between *syn*-F or *anti*-F nuclei increase from γ-lactam to thioamide and amidine counterparts.

In both γ-lactam and thioamide derivatives (*i.e.*, **1b–e** and **2b–e**), ^{19}F shift differences $\Delta\delta$ increase when the C9-substituent changes from CO_2Me to $CONH_2$, CONHMe and $CONMe_2$ groups. Obviously, C9-substituents modulate *ortho*-F shielding in addition to C7-functional groups. The combination of the most polarizable groups at both C7- and C9-sites, *i.e.*, C7–C=S and C9–$CONMe_2$, results in compound **2e** displaying the largest chemical shift difference $\Delta\delta$ at 2.56 ppm. This result may be applicable to the design of molecular sensors, in which the purposely formed polarizable groups will expand ^{19}F shift changes.

© 2022 The Author(s). Published by the Royal Society of Chemistry

Open Access Article. Published on 09 November 2022. Downloaded on 2/10/2026 6:58:20 PM.
This article is licensed under a Creative Commons Attribution-NonCommercial 3.0 Unported Licence.

Table 2 ^{19}F NMR chemical shifts δ_{down} and δ_{up}, shift differences $\Delta\delta$ for amidines **3a–e** and **4a–r** (in ppm)[a]

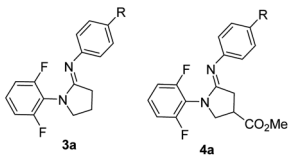

Cpd	R	$\delta_{down}^{amidine}$	$\delta_{up}^{amidine}$	$\Delta\delta^{amidine}$	σ_{para}
3a	H	−117.05	—	0	0
3b	Me	−117.06	—	0	−0.17
3c	OMe	−117.07	—	0	−0.27
3d	CF_3	−117.18	—	0	0.54
3e	NO_2	−117.30	—	0	0.78
4a	H	−116.31	−117.41	1.09	0
4b	Me	−116.26	−117.41	1.15	−0.17
4c	OMe	−116.31	−117.42	1.11	−0.27
4d	CF_3	−116.49	−117.47	0.98	0.54
4e	NO_2	−116.65	−117.48	0.83	0.78
4f	NMe_2	−116.17	−117.37	1.20	−0.83
4g	OEt	−116.33	−117.42	1.09	−0.24
4h	F	−116.46	−117.47	1.01	0.06
4i	Cl	−116.46	−117.46	1.00	0.23
4j	Br	−116.46	−117.46	1.00	0.23
4k	I	−116.44	−117.44	1.00	0.18
4l	CN	−116.61	−117.48	0.87	0.66
4m	CHO	−116.53	−117.45	0.92	0.42
4n	COMe	−116.47	−117.42	0.94	0.5
4o	CO_2Me	−116.49	−117.46	0.97	0.45
4p	$CONMe_2$	−116.40	−117.42	1.01	—
4q	NHCOMe	−116.34	−117.40	1.06	0
4r	$CH_2{=}CH_2$	−116.33	−117.41	1.08	−0.02

[a] $\Delta\delta^{amidine} = \delta_{down}^{amidine} - \delta_{up}^{amidine}$; σ_{para} is Hammett constants for *para*-substituents.

The C7-thioamide and the phenyl group in C7-amidines bring different electronic and steric influences on the pyrrolidine ring as compared to C7–C=O group. The subtle conformational differences among these compounds are manifested in the crystal structures of **2a**, **3a** and **5a**, which we determined by X-ray crystallography. As revealed in Fig. S1,† the pyrrolidine ring in **2a** and **3a** displays similar puckered conformations with C9 extruding out of the plane, in contrast to near flat γ-lactam ring in **5a**.[15] The torsion angles for **2a**, **3a** and **5a** are 81.56°, 65.31° and 62.63°, respectively, correlating to the increasing bulkiness of thioamide, amidine and amide groups. Meanwhile, the two phenyl groups in **3a** adopts *trans*-configuration. Hence, the effects of various *para*-substituted phenylamidines on ^{19}F chemical shifts are mostly instigated by electrostatic rather than steric effects. To evaluate the influences of C7-amidines on ^{19}F shielding, we prepared compounds **3b–e** and **4b–q**. Table 2 compiles their ^{19}F chemical shifts and shift differences $\Delta\delta$ between the *syn*-F and *anti*-F, along with Hammett constants σ_{para}.

As expected, achiral compounds **3a–e** furnish convergent ^{19}F signals for *ortho*-F nuclei. Electron-rich amidines **3b–c** show deshielded ^{19}F nuclei as compared to electron-deficient **3d–e**.

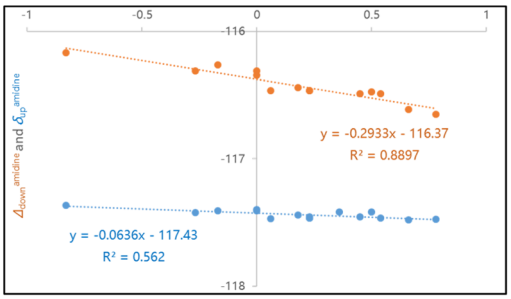

Fig. 6 Hammett plots of ^{19}F chemical shifts and shift differences *versus* σ_{para}: (a) $\delta_{down}^{amidine}$–σ_{para} curve; (b) $\delta_{up}^{amidine}$–σ_{para} curve (κ represents the slope coefficient).

Close examination on divergent ^{19}F chemical shifts in chiral compounds **4a–q** shows that this "reverse" relationship between ^{19}F shielding and electron-withdrawing abilities maintains.[16] In fact, linear correlations of *ortho*-^{19}F chemical shifts with Hammett constants σ_{para} is seen in Hammett plots, as illustrated in Fig. 6. The negative slope coefficient κ indicates that amidine groups affect ^{19}F shielding predominately through noncovalent interaction, not chemical bonds for both *syn*-F and *anti*-F nuclei. Notably, the slope coefficient ($\kappa = -0.29$) for δ_{down}–σ_{para} curve is bigger (in absolute value) than that for δ_{up}–σ_{para} plot ($\kappa = -0.06$). Larger *syn*-^{19}F chemical shift (δ_{down}) changes are likely originated from cooperative effects of nonbonding interactions of *syn*-F nucleus with C9-ester and C7-amidine.

2.3. C5-substituent effects on ^{19}F chemical shifts

In C7- and C9-substituted molecules, the electronic properties of F nuclei are little affected. Alternatively, substituent changes on the *N*-phenyl ring allow us to modulate fluorine electronic properties. Any different responses of *syn*-F and *anti*-F to C5-substituent variations reflect the electronic effects of fluorine on nonbonding interactions. To that end, we prepared a series

Table 3 ^{19}F Chemical shifts and shift differences in *para*-substituted *N*-phenyl γ-lactam compounds (in ppm)

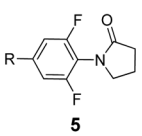

5

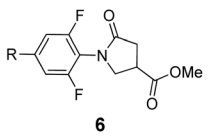

6

Cpd	R	σ_{meta}	δ_{ref}^{meta}	Cpd	δ_{down}	δ_{up}	$\Delta\delta^{meta}$
1a	H	0	−117.82	**1b**	−117.14	−117.93	0.79
5a	Me	−0.07	−119.21	**6a**	−118.56	−119.35	0.79
5b	OMe	0.115	−117.42	**6b**	−116.75	−117.61	0.86
5c	CF_3	0.43	−113.36	**6c**	−112.73	−113.43	0.70
5d	NO_2	0.71	−110.99	**6d**	−110.57	−110.90	0.33
5e	CO_2Me	0.37	−115.34	**6e**	−114.78	−115.42	0.64
5f	NH_2	−0.16	−119.53	**6f**	−118.89	−119.70	0.81
5g	NHMe	−0.21	−119.85	**6g**	−119.31	−120.10	0.79
5h	NMe_2	−0.15	−119.45	**6h**	−118.84	−119.67	0.83
5i	F	0.337	−114.61	**6i**	−113.93	−114.72	0.79

© 2022 The Author(s). Published by the Royal Society of Chemistry

Open Access Article. Published on 09 November 2022. Downloaded on 2/10/2026 6:58:20 PM.
This article is licensed under a Creative Commons Attribution-NonCommercial 3.0 Unported Licence.

Table 4 ^{19}F Chemical shifts and shift differences in *para*-substituted *N*-phenyl γ-lactam compounds **6j–6w** (in ppm)

Cpd	R	σ_{meta}	δ_{down}; δ_{up}	$\Delta\delta^{meta}$
6j	Cl	0.373	−114.90, −115.58	0.68
6k	Br	0.39	−114.94, −115.73	0.788
6l	I	0.35	−115.44, −116.20	0.768
6m	Et	−0.07	−118.28, −119.07	0.798
6n	*n*-Pr	−0.07	−118.39, −119.16	0.77
6o	OEt	0.10	−117.02, −117.89	0.86
6p	CH_2=CH_2	0.05	−117.42, −118.16	0.74
6q	CH_2=CHMe	0.05	−117.98, −118.75	0.77
6r	Ph	0.06	−116.85, −117.62	0.77
6s	CHO	0.35	−113.13, −113.72	0.59
6t	COMe	0.38	−114.25, −114.86	0.61
6u	CN	0.56	−111.95, −112.30	0.35
6v	NHCHO	0.19	−117.46, −117.98	0.52
6w	NHCOMe	0.21	−118.54, −119.11	0.57

of C5-substituted *N*-phenyl derivatives **5a–h** and **6a–w** (*meta*-substituent relative to *ortho*-F nuclei, see Fig. 1) and examined their ^{19}F NMR spectra. Tables 3 and 4 provide detailed ^{19}F chemical shifts for **5a–h** and **6a–w**.

We expect that through-bond forces such as induction and resonance effects would be leading factors for C5-substituents to affect ^{19}F chemical shifts. Indeed, plots of ^{19}F chemical shifts δ from **5a–h**, δ_{down} and δ_{up} from **6a–u** *versus* Hammett constants σ_{meta} exhibit linear relationships, as demonstrated in 8 and S2.† The positive slope coefficients κ in the curves are in consistent with the conventional Hammett plots. Thus, ^{19}F shielding variations in C5-substituted γ-lactams are predominately governed by either through-bond effects. It is worth to note that the chemical shifts of C5-amides **6v** (R = NHCHO) and **6w** (R = NHCOMe) are distinctly deviated from the linear curves, which we attribute to strong amide polarizable effects and their data are omitted from the plots in Fig. 7.

We envision that the magnitude of slope coefficient κ in a Hammett plot indicates the susceptibility of ^{19}F shifts to substituent electronic characteristics. The slope coefficients for δ_{down}–σ_{meta} plots of C5-substituted γ-lactams (κ = 9.45 in Fig. 7) are much bigger than those for δ_{down}–σ_{para} plots of C7-amidines (κ = −0.29 in Fig. 6), proving that through-bond forces have greater impacts on ^{19}F shielding than through-space interactions. In addition, the *syn*-F and *anti*-F nucleus behave

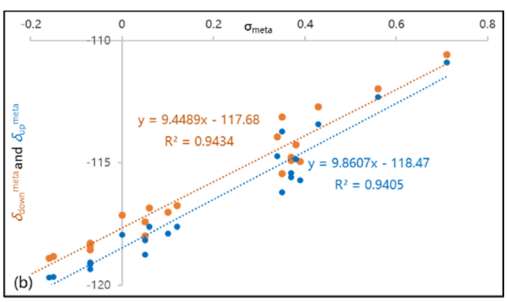

Fig. 7 Hammett plots of δ_{down}–σ_{meta} and δ_{up}–σ_{meta} for compounds **6a–w**.

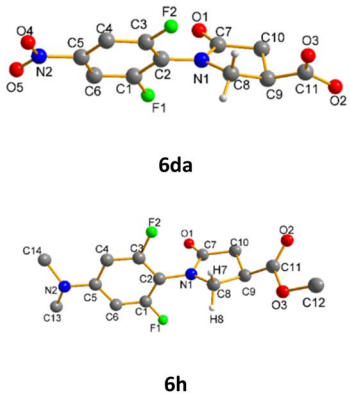

Fig. 8 Computer-generated drawings of crystal structures **6da** and **6h**. **6da** is a C9-acid analogue of **6d**.

differently in responding to their discrete surroundings, as the slope for δ_{down}–σ_{meta} plot (κ = 9.45) is smaller than that of δ_{up}–σ_{meta} curve (κ = 9.86). The asymmetric environments around *anti*-F and *syn*-F nuclei are shaped by not only C9-ester but also neighboring C7-amidine. *Anti*-F shielding is more sensitive to the changes of fluorine electronic property than *syn*-F, suggesting *anti*-F is closer to C7-amidine that *syn*-F. Thus, for the first time, we demonstrate that the slope coefficients in Hammett plots are useful in detecting the type and strength of fluorine involved bonding and nonbonding interactions.

2.4. X-ray crystal structures of C5-substituted *N*-phenyl γ-lactams

In *N*-phenyl γ-lactam derivatives, the asymmetric chemical environments around *ortho*-F nuclei are mainly regulated by C9-ester and neighboring C=O/CH_2 groups. The conjugation effects of C5-substituents hinder rotations around central N–Ph bond, enlarging chemical differences between *syn*-F and *anti*-F. To inspect the structural details of C5-substituted *N*-phenyl γ-lactams, we determined single crystal structures of **6da** (C9-acid derivative of **6d**) and **6h** by X-ray crystallography. Fig. 8 shows computer generated drawings with atomic numbering for *S*-**6da** and *R*-**6h**. Table 4 lists parameters that define important atom distances and functional group orientations. CCDC 1904410 and 1915197 contain the supplementary crystallographic data for **6da** and **6h**, respectively.†

As shown in Table 5, *S*-**6da** displays a small torsion angles ϕ at 57.59° due to C5–NO_2 resonance effects, affording strong van der Waals forces between F2···C=O ($d_{F2–O1}$ = 2.83 Å) and F1···CH_2 ($d_{F1–H8}$ = 2.45 Å). F2 is *anti*-F relative to equatorial C9-acid in *S*-**6da**. On the contrary, C5NMe_2 *R*-**6h** has larger torsion angle ϕ of 76.54° and longer distances from *ortho*-F nuclei to the nearby groups. None of the *syn*-F and *anti*-F nuclei approach to the C=O/CH_2 groups within the sum of van der Waals radius in *R*-**6h**. Despite marked differences in *N*-Ph torsion angles, C9-substituents in both *S*-**6da** and *R*-**6h** occupy similar pseudo-equatorial orientations, suggesting that there is no direct correlation between torsion angle ϕ and C9-substituent orientation. Significantly, strong nonbonding interactions as

© 2022 The Author(s). Published by the Royal Society of Chemistry

Open Access Article. Published on 09 November 2022. Downloaded on 2/10/2026 6:58:20 PM. This article is licensed under a Creative Commons Attribution-NonCommercial 3.0 Unported Licence.

Table 5 Selected atom distances, dihedral angles, and torsion angles in the crystal structures of **6da** and **6h**[a]

Parameter		*S*-**6da**	*R*-**6h**
Dihedral angle β (carbonyl orientation)	β_1[C7–C10–C9–C11]	−150.45	−145.27
	β_2[N1–C8–C9–C11]	150.85	148.21
Torsion angle ϕ (between N–Ph and γ-lactam)	ϕ_1[C1–C2–N1–C7]	−124.13	99.77
	ϕ_2[C3–C2–N1–C7]	57.59	−76.54
Contact angle α (F to C=O groups)	α_1[C3–F2–C(amide)]	82.34	74.07
	α_2[F2–C=O]	71.08	91.45
	α_1[C1–F1–C(amide)]	66.91	70.44
	α_2[F1–C=O]	112.91	94.14
Distances d (F to C=O and CH_2 groups)	$d_{F1–C8(CH)}$	2.903	3.609
	$d_{F1–H8(CH)}$	**2.446**	3.324
	$d_{F1–O1(amide)}$	4.470	3.877
	$d_{F1–C7(amide)}$	3.851	3.592
	$d_{F2–C8(CH)}$	3.946	3.386
	$d_{F2–H7(CH)}$	3.994	2.996
	$d_{F2–O1(amide)}$	**2.826**	3.478
	$d_{F2–C7(amide)}$	2.975	3.226
C–F bond lengths	$d_{C1–F1}$	1.343	1.359
	$d_{C3–F2}$	1.340	1.356
Distances of F to C9-carbonyl	$d_{F2–O2}$ (F to axial carbonyl)	6.663	5.536
	$d_{F2–C11}$ (F to axial carbonyl)	5.991	5.165
	$d_{F1–O3}$ (F to axial carbonyl)	4.783	6.178
	$d_{F1–C11}$ (F to axial carbonyl)	5.028	5.895

[a] Sum of van der Waals radii: $R_{w(F–C)} = 3.17$ Å; $R_{w(F–O)} = 2.99$ Å; $R_{w(F–H)} = 2.67$ Å.

exemplified in structure *S*-**6da** correlates to small shift differences $\Delta\delta$ (Tables 3 and 4).

2.5. Quantum mechanics calculation on nonbonding interactions between *ortho*-F nuclei and neighboring C=O/C=N/CH_2 groups

Having a wealth of valuable geometric and ^{19}F NMR spectroscopic information in hand, we set to explore the nature of the interactions between *ortho*-F nuclei and neighboring C=O/C=N/CH_2 groups. We first carried out geometry optimizations using the Gaussian16 program with density functional theory (DFT) at the B3LYP/6-311G* level of theory.[23] We analyzed LUMO, HOMO and HOMO−1 orbitals in amide **1b**, thioamide **2b** and amidine **4a**, and their molecular orbitals are depicted inFig. 9 and S3.†

Fluorine nonbonding interactions are multifaceted. In our model molecules **1–6**, interactions such as van der Waals contacts, coulombic (electrostatic and polarization), and orbital delocalization play important roles in governing overall conformation, and affecting ^{19}F NMR chemical shifts.[24–26] It is known that lone pair electrons (n) on F can delocalize to the antibonding orbital (π*) of the adjacent C=O group from the C end.[25a] However, *ortho*-F nucleus can only approach to C=O group sideways in γ-lactam derivatives due to conformational confinement. In fact, HOMO and LUMO orbitals in **1b** suggest that there is repulsive interaction between p-type lone pair electrons on F and O atoms (coulombic n ↔ n repulsive interactions). On the other hand, the same *ortho*-F nucleus also engages n → π* orbital overlaps through donation of n electrons on F into antibonding π* orbitals in N=Ph* tautomeric form (Ph* denotes the *ortho*-F substituted phenyl group). This attractive contact offsets F···O repulsion and favors small torsion angle.

The interaction of lone pair electrons between *ortho*-F and S, however, is not apparent in thioamide **2b**, as the van der Waals repulsive force between the *ortho*-F and large S atom dominates, furnishing a large torsion angle (*vide supra*).

Notably, a π* orbital located between N and the attaching phenyl group (*i.e.*, N=Ar, a tautomer of phenylamidine, see Fig. 9) exists. Unlike repelling C–F···O=C interaction in γ-lactam **1b**, the obvious n → π* orbital delocalization from lone

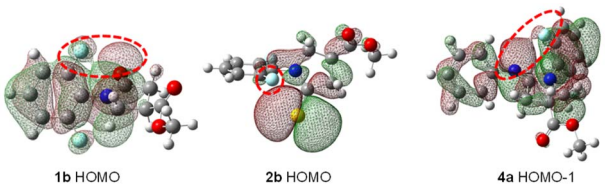

Fig. 9 Molecular orbitals at HOMO energy levels in amide **1b**, thioamide **2b**, and HOMO−1 in amidine **4a** (on 0.012 e au^{-3} electron density surface).

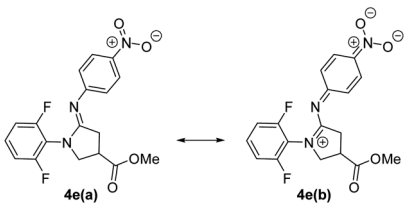

Fig. 10 Tautomers of amidine **4e**.

Open Access Article. Published on 09 November 2022. Downloaded on 2/10/2026 6:58:20 PM.
This article is licensed under a Creative Commons Attribution-NonCommercial 3.0 Unported Licence.

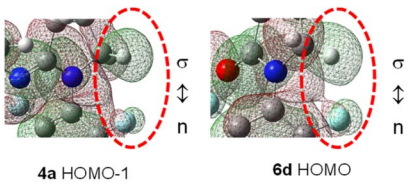

Fig. 11 HOMO−1 orbital in amidine **4a** and HOMO orbital in C5–NO_2 γ-lactam **6d** (on 0.012 e au^{-3} electron density surface, C–F···H–C portion).

pair electrons (n) on F to the antibonding orbital π* in N=Ar is deemed to stabilize C–F···N=Ar contact, although the attraction energy may be small.[2,25,28] Accordingly, *para*-NO_2 amidine **4e** furnishes better n → π* orbital overlap than that of *p*-NMe_2 amidine **4f**, as **4e** majorly adopts Ar=N form **4e**(b), (see Fig. 10 and S3†).

C–F···H–C contacts in amidines **4** are little affected by the *p*-substituents, but are more likely influenced by C5-substituents in γ-lactams **6**. Indeed, molecular orbital analysis of **4a** indicates that lone pair electrons (n) on F clash sideway into the proximate C–H σ bonding orbital (n ↔ σ interaction, Fig. 11 and S4†).[27] Since both orbitals are occupied, such a F···H interaction is repulsive, and the short F···H distance is a consequence of steric crowding (buttressing), rather than any meaningful hydrogen bonding interaction.[14] Strong F···H van der Waals repulsion is anticipated in C5–NO_2-γ-lactam **6d**, where C5-conjugation effect shortens the F···H distance (Fig. 11and S4†). However, orbital polarization between n and σ orbitals in **6d** seems insignificant, partly because fluorine is electron-deficient and less polarizable.

2.6. Fluorine nonbonding interactions and ^{19}F NMR chemical shift changes

Through-space interactions between *ortho*-F nuclei and their surrounding groups may be measured by shift differences $\Delta\delta_{down}$ (for *syn*-F) and $\Delta\delta_{up}$ (for *anti*-F) *versus* a corresponding reference chemical shift (δ_{ref}). Here we use C9-unsubstituted γ-lactams **5a–i** as references for **6a-I**, and achiral amidines **3a–e** as references for **4a–e**. Values of $\Delta\delta_{down}$ ($=\delta_{down} - \delta_{ref}$) and $\Delta\delta_{up}$ ($=\delta_{up} - \delta_{ref}$) reflects substituent effects on ^{19}F NMR chemical shifts for F···O=C/N=C and F···H–C interactions, respectively. Table 6 lists $\Delta\delta_{down}$ and $\Delta\delta_{up}$ data for selected amidines and γ-lactams.

Previously we established that ^{19}F shielding variations correlate with dipole moments/polarizability in C–F···O=C interactions.[15,16] Our molecular orbital analysis confirms that ^{19}F NMR signals are mostly affected by functional group polarity, where ^{19}F chemical shifts are more deshielded when either F nucleus or C=O/Ar=N groups become more polarizable. As detailed in Table 6, *ortho*-F nuclei are more polarizable in C5–NMe_2 γ-lactam **6h** than in C5–NO_2 **6d**, leading to larger $\Delta\delta_{down}$ for **6h** (0.61 ppm) than for **6d** (0.42 ppm).

In C–F···H–C interactions, short F···H distances are associated with deshielded ^{19}F signals (Table 6). Thus, upfield ^{19}F signal δ_{up} in **6d** displays the most downfield shift value ($\Delta\delta_{up}$ = 0.09 ppm), which is associated with the shortest $d_{F-H} = 2.45$ Å in γ-lactams. Similar correlation between $\Delta\delta_{up}$ and d_{F-H} is observed in amidine series, and documented in literature.[14]

Table 6 ^{19}F Chemical shift differences $\Delta\delta_{down}$ and $\Delta\delta_{up}$ for amidines **4a–d**, *N*-phenyl γ-lactams **6a–d** and **6h** (in ppm)

Cpd	R	$\Delta\delta_{down}$	$\Delta\delta_{up}$	d_{F-H}[a] (Å)
4a	H	0.74	−0.36	2.550
4b	Me	0.80	−0.35	2.550
4c	OMe	0.76	−0.35	2.550
4d	CF_3	0.69	−0.29	2.538
4e	NO_2	0.65	−0.18	2.548
1b	H	0.68	−0.11	2.518
6a	Me	0.65	−0.14	2.585
6b	OMe	0.67	−0.19	2.639
6c	CF_3	0.63	−0.07	2.508
6d	NO_2	0.42	0.09	2.446[b]
6h	NMe_2	0.61	−0.22	3.324[b]

[a] F···H distances are obtained from optimized structures from QM calculations. [b] Data are from X-ray crystal structures.

3. Conclusions

In this work, we investigated the relationship between ^{19}F NMR shielding changes and chemical environments in rotameric *N*-phenyl γ-lactam analogues. ^{19}F shift changes in C7-amide/thioamide/amidine derivatives **1–3** confirmed that the neighboring C=O/C=S/C=N and CH_2 groups, together with stereogenic C9-substituent on γ-lactam ring, synergistically enhance chemical environment differences between *syn*-F and *anti*-F. Substituent surveys among C7-phenylamidines **4a–r** and C5-substituted γ-lactams **6a–u** revealed that through-bond effects track conventional relationships between ^{19}F chemical shift (δ) and Hammett coefficient (σ), while through-space interactions display "reverse" correlations in δ–σ Hammett plots. In fact, the signs (positive or negative) of the slope coefficients κ in the Hammett plots specify the types of fluorine-participated molecular recognitions.

The absolute values of slope coefficients κ in δ–σ Hammett plots verified that nonbonding contacts ($\kappa = -0.29$ for F···N=Ar contacts) are much weaker than bonding interactions in amending ^{19}F shielding (Fig. 6 and 7). Such results corroborated with our earlier observations from C9-amides series,[16] where the nonbonding effects of C9-amides on ^{19}F shielding afforded $\kappa = -0.35$ in the δ_{down}–σ_{para} Hammett plot. To the best of our knowledge, this is the first report to show that Hammett plots can be used to categorize fluorine nonbonding interactions, and to explicitly gauge the magnitude of these interactions using the slope coefficients κ from Hammett plots.

QM calculations established that repulsive interactions between F···O=C and F···H–C are the main schemes in *N*-phenyl γ-lactams, while a favorable, n → π* orbital delocalization from lone pair electrons (n) on F into Ar=N antibonding orbital π* exists in amidine analogous. All the orbital overlaps are supposed to be weak interactions. It is evident that more polarizable functional groups link to more deshielded ^{19}F

© 2022 The Author(s). Published by the Royal Society of Chemistry

Open Access Article. Published on 09 November 2022. Downloaded on 2/10/2026 6:58:20 PM.
This article is licensed under a Creative Commons Attribution-NonCommercial 3.0 Unported Licence.

signals. On the other hand, C–F···H–C interaction comprises orbital polarizations between lone pair electrons on F and C–H σ bonding orbital (n ↔ σ). As both n and σ orbitals are occupied, this contact is considered steric repulsive, and is associated with ^{19}F signal deshielding.

4. Experimental section

4.1. General information

Unless otherwise stated, all the reactions were carried out under atmosphere conditions. All chemical reagents were purchased from commercial sources and used without further purification. Flash column chromatography was performed with Agilent Technologies Claricep FlashSilica. All ^{1}H and ^{13}C NMR experiments were carried out using a Bruker AVANCE 400 spectrometer or a Bruker AVANCE III 600 spectrometer. ^{19}F NMR data was recorded using a Bruker AVANCE 400 spectrometer. Chemical shifts in ^{1}H, ^{19}F and ^{13}C NMR spectra were reported in parts per million (ppm). The residual solvent signals were used as references and the chemical shifts converted to the TMS scale ($CDCl_3$: δ (H) = 7.26 ppm, δ (C) = 77.16 ppm) for ^{1}H and ^{13}C NMR spectra. For ^{19}F NMR experiments, $CFCl_3$ was added as an internal reference (0.5% $CFCl_3$). All coupling constants (J values) were reported in Hertz (Hz). Multiplicities were reported as follows: singlet (s), doublet (d), doublet of doublets (dd), doublet of doublet of doublets (ddd), doublet of triplets (dt), triplet (t), triplet of doublets (td), quartet (q), and multiplet (m). High resolution mass spectra (HRMS) were obtained from an Agilent 6200 series TOF/6500 series spectrometer, using electrospray ionization (ESI) as an ion source. The MS spectra were assessed with an Agilent 1260-6120 spectrometer with an electrospray ionization (ESI) source, equipped with an Agilent SB-C18 (2.1 × 30 mm, 3.5 μm) column.

4.2. Compound characterization

4.2.1. General procedure for the synthesis of compounds 2a and 2b. To a solution of compound **1a** (197 mg, 1.00 mmol) in THF (2 mL) was added Lawesson's reagent (202 mg, 0.50 mmol). The mixture was stirred at room temperature for 5 h. The reaction was quenched with saturated $NaHCO_3$ solution (10 mL), then extracted with dichloromethane (10 mL × 3). The combined organic phases were washed with brine (20 mL), dried over anhydrous Na_2SO_4 and concentrated *in vacuo*. The residue was purified by a flash column chromatography (EtOAc/PE (v/v) = 1/10 to 1/1) to give compound **2a** (123 mg, 51%) as pale yellow oil. MS (ESI, pos. ion) m/z: 214.4 $[M + H]^+$; ^{1}H NMR (400 MHz, $CDCl_3$): δ (ppm) 7.41–7.32 (m, 1H), 7.03 (t, J = 8.2 Hz, 2H), 4.00 (t, J = 7.2 Hz, 2H), 3.20 (t, J = 7.9 Hz, 2H), 2.39–2.28 (m, 2H); ^{19}F NMR (376 MHz, $CDCl_3$): δ (ppm) −117.49 (s); ^{13}C NMR (101 MHz, $CDCl_3$): δ (ppm) 206.1, 158.3 (dd, $^{1}J_{CF}$ = 253.8, 5.0 Hz), 130.2 (t, $^{3}J_{CF}$ = 9.8 Hz), 117.6 (t, $^{3}J_{CF}$ = 16.3 Hz), 112.6–112.2 (m), 57.0, 44.5, 21.6; HRMS (ESI-TOF) m/z: $[M + H]^+$ calcd for $C_{10}H_{10}F_2NS$ 214.0502; found: 214.0494.

Compound **2b**: 133 mg, 58%, pale yellow oil. MS (ESI, pos. ion) m/z: 272.4 ($[M + H]^+$); ^{1}H NMR (400 MHz, $CDCl_3$): δ (ppm) 7.43–7.33 (m, 1H), 7.03 (t, J = 8.4 Hz, 2H), 4.23 (ABX, J = 10.7, 6.4, 8.4 Hz, 2H), 3.79 (s, 3H), 3.60–3.50 (m, 1H), 3.48–3.46 (m, 2H);^{19}F NMR (376 MHz, $CDCl_3$): δ (ppm) −116.53 (s), −117.69 (s); ^{13}C NMR (101 MHz, $CDCl_3$): δ (ppm) 203.1, 172.1, 158.3 (dt, $^{3}J_{CF}$ = 9.3, 5.0 Hz), 130.6 (t, $^{3}J_{CF}$ = 9.8 Hz), 116.8 (t, $^{3}J_{CF}$ = 16.1 Hz), 112.8–112.1 (m), 58.1, 52.8, 46.9, 39.4; HRMS (ESI-TOF) m/z: $[M + H]^+$ calcd for $C_{12}H_{12}F_2NO_2S$ 272.0557; found: 272.0550.

4.2.2. General procedure for the synthesis of compounds 2c, 2d and 2e. To a solution of compound **2b** (100 mg, 0.37 mmol) in 1,4-dioxane (2 mL) was added a LiOH (2 mL, 2 mol L^{-1} in water). The mixture was stirred at 50 °C for 8 h. The reaction was cooled to room temperature, adjusted to pH = 2 with conc. HCl aqueous solution, then extracted with dichloromethane (10 mL × 3). The combined organic phases were washed with brine (20 mL), dried over anhydrous Na_2SO_4 and concentrated *in vacuo*. The residue was purified by a flash column chromatography (EtOAc/PE (v/v) = 1/50 to 2/1) to give compound **2f** (88 mg, 93%) as pale yellow oil. MS (ESI, pos. ion) m/z: 258.2 ($[M + H]^+$); ^{1}H NMR (400 MHz, $CDCl_3$): δ (ppm) 7.82 (brs, 1H), 7.45–7.33 (m, 1H), 7.04 (t, J = 8.5 Hz, 2H), 4.32 (dd, J = 10.7, 6.0 Hz, 1H), 4.20 (t, J = 9.6 Hz, 1H), 3.67–3.56 (m, 1H), 3.51 (d, J = 7.6 Hz, 2H); ^{19}F NMR (376 MHz, $CDCl_3$): δ (ppm) −115.56 (s), −117.59 (s); ^{13}C NMR (151 MHz, $CDCl_3$): δ (ppm) 202.8, 177.3, 158.3 (ddd, $^{3}J_{CF}$ = 11.1, 6.8, 5.1 Hz), 130.7 (t, $^{3}J_{CF}$ = 9.7 Hz), 116.7 (t, $^{3}J_{CF}$ = 16.1 Hz), 112.6 (td, $^{3}J_{CF}$ = 20.0, 3.3 Hz), 57.8, 46.7, 39.3; HRMS (ESI-TOF) m/z: $[M + H]^+$ calcd for $C_{11}H_{10}F_2NO_2S$ 258.0400; found: 258.0391.

To a solution of compound **2f** (200 mg, 0.78 mmol), aniline (1.00 equiv.) and HATU (443 mg, 1.17 mmol) in dichloromethane (30 mL) was added Et_3N (118 mg, 1.17 mmol). The mixture was stirred at room temperature for 8 h. The reaction was quenched with water (30 mL), then extracted with dichloromethane (30 mL × 3). The combined organic phases were washed with brine (30 mL), dried over anhydrous Na_2SO_4 and concentrated *in vacuo*. The residue was purified by a flash column chromatography (EtOAc/PE (v/v) = 1/10 to 1/1) to give compounds **2c**, **2d** and **2e**.

Compound **2c** (100 mg, 50%) as pale yellow oil. MS (ESI, pos. ion) m/z: 257.1 ($[M + H]^+$); ^{1}H NMR (400 MHz, $CDCl_3$): δ (ppm) 7.41–7.32 (m, 1H), 6.99 (t, J = 8.5 Hz, 2H), 5.79 (d, J = 57.9 Hz, 2H), 4.01 (dd, J = 9.4, 7.5 Hz, 1H), 3.88 (t, J = 9.0 Hz, 1H), 3.45–3.31 (m, 1H), 2.85 (ABX, J = 10.7, 6.4, 8.4 Hz, 2H); ^{19}F NMR (376 MHz, $CDCl_3$): δ (ppm) −116.81 (s), −118.15 (s); ^{13}C NMR (101 MHz, $CDCl_3$): δ (ppm) 173.6, 172.4, 159.1 (dd, $^{1}J_{CF}$ = 253.0, $^{3}J_{CF}$ = 4.9 Hz), 129.5 (t, $^{3}J_{CF}$ = 9.9 Hz), 115.0 (t, $^{3}J_{CF}$ = 16.4 Hz), 112.3 (d, $^{2}J_{CF}$ = 21.8 Hz), 51.4, 38.6, 34.2; HRMS (ESI-TOF) m/z: $[M + H]^+$ calcd for $C_{11}H_{11}F_2N_2OS$ 257.0560; found: 257.0547.

Compound **2d** (120 mg, 57%) as pale yellow oil. MS (ESI, pos. ion) m/z: 271.0 ($[M + H]^+$); ^{1}H NMR (400 MHz, $CDCl_3$): δ (ppm) 7.37 (dq, J = 8.5, 6.2 Hz, 1H), 7.01 (tt, J = 12.8, 6.4 Hz, 2H), 6.15 (brs, 1H), 4.35–4.26 (m, 1H), 4.11–4.02 (m, 1H), 3.46–3.33 (m, 3H), 2.83 (d, J = 4.8 Hz, 3H); ^{19}F NMR (376 MHz, $CDCl_3$): δ (ppm) −116.10 (s), −118.07 (s); ^{13}C NMR (151 MHz, $CDCl_3$): δ (ppm) 203.5, 171.5, 158.2 (ddd, $^{2}J_{CF}$ = 22.6, $^{3}J_{CF}$ = 18.5, 4.9 Hz), 130.6 (t, $^{3}J_{CF}$ = 9.7 Hz), 116.8 (t, $^{3}J_{CF}$ = 16.1 Hz), 112.5 (ddd, $^{2}J_{CF}$ = 33.3, $^{3}J_{CF}$ = 19.5, 3.3 Hz), 59.0, 48.0, 41.2, 26.7; HRMS (ESI-TOF) m/z: $[M + H]^+$ calcd for $C_{12}H_{13}F_2N_2OS$ 271.0717; found: 271.0704.

Open Access Article. Published on 09 November 2022. Downloaded on 2/10/2026 6:58:20 PM. This article is licensed under a Creative Commons Attribution-NonCommercial 3.0 Unported Licence.

Compound **2e** (140 mg, 63%) as pale yellow oil. MS (ESI, pos. ion) *m*/*z*: 285.1 ([M + H]$^+$); ^{1}H NMR (400 MHz, $CDCl_3$): δ (ppm) 7.34 (tt, J = 8.5, 6.2 Hz, 1H), 7.00 (ddd, J = 9.3, 3.6, 1.3 Hz, 2H), 4.45 (dd, J = 10.3, 7.7 Hz, 1H), 4.01 (dd, J = 10.2, 8.8 Hz, 1H), 3.82–3.70 (m, 1H), 3.47–3.29 (m, 2H), 3.05 (s, 3H), 2.97 (s, 3H); ^{19}F NMR (376 MHz, $CDCl_3$): δ (ppm) −115.59 (s), −118.16 (s); ^{13}C NMR (101 MHz, $CDCl_3$): δ (ppm) 202.9, 170.3, 158.2 (ddd, $^3J_{CF}$ = 17.3, 13.7, 4.8 Hz), 130.4 (t, $^3J_{CF}$ = 9.8 Hz), 116.9 (t, $^3J_{CF}$ = 16.2 Hz), 112.4 (ddd, $^2J_{CF}$ = 30.5, $^3J_{CF}$ = 19.6, 3.5 Hz), 58.64, 47.6, 38.6, 37.5, 37.2, 36.0; HRMS (ESI-TOF) *m*/*z*: [M + H]$^+$ calcd for $C_{13}H_{15}F_2N_2OS$ 285.0873; found: 285.0864.

4.2.3. General procedure for the synthesis of compounds 3a–3e and 4a–4e. Phosphorus oxychloride (1.03 g, 6.72 mmol) was added dropwise to a solution of compound **1a** (1.54 g, 7.81 mmol) in dry dichloromethane (5.0 mL) and the reaction mixture was stirred for 3 h at room temperature. A solution of aniline (500 mg, 5.34 mmol) in dry dichloromethane (15 mL) was then added *via* cannula and the mixture was refluxed overnight. Then, the reaction mixture was cooled to room temperature and concentrated *in vacuo*. The resulting solid was dissolved in aqueous hydrochloric acid (0.30 M, 100 mL) and extracted with dichloromethane (100 mL × 3). The aqueous phase was basified with sodium hydroxide aqueous solution (2.0 M, pH adjusted to 8) and extracted with ethyl acetate (100 mL × 3). The first organic extracts were concentrated *in vacuo* and the resulting solid was carried through the above procedure three more times. All ethyl acetate extracts were combined, dried over anhydrous Na_2SO_4 and concentrated *in vacuo*. The residue was purified by a flash column chromatography (EtOAc/PE (v/v) = 1/10 to 1/4) to give compound **3a** (615 mg, 30%) as colorless oil. MS (ESI, pos. ion) *m*/*z*: 273.1 ([M + H]$^+$); ^{1}H NMR (400 MHz, $CDCl_3$): δ (ppm) 7.25–7.16 (m, 3H), 7.02–6.91 (m, 3H), 6.83–6.81 (m, 2H), 3.70 (t, J = 6.8 Hz, 2H), 2.51 (t, J = 7.8 Hz, 2H), 2.19–2.12 (m, 2H); ^{19}F NMR (376 MHz, $CDCl_3$): δ (ppm) −117.05 (s); ^{13}C NMR (151 MHz, $CDCl_3$): δ (ppm) 161.5, 159.7 (dd, $^1J_{CF}$ = 252.0, $^3J_{CF}$ = 5.6 Hz), 152.2, 128.7, 128.1 (t, $^3J_{CF}$ = 10.0 Hz), 122.3, 122.2, 112.3 (dd, $^3J_{CF}$ = 19.7, 4.1 Hz), 50.8, 26.9, 21.4; HRMS (ESI-TOF) *m*/*z*: [M + H]$^+$ calcd for $C_{16}H_{15}F_2N_2$ 273.1203; found: 273.1198.

Compound **3b**: 630 mg, 41%, yellow oil. MS (ESI, pos. ion) *m*/*z*: 287.2 ([M + H]$^+$); ^{1}H NMR (400 MHz, $CDCl_3$): δ (ppm) 7.25–7.15 (m, 1H), 7.02 (d, J = 8.0 Hz, 2H), 6.96 (t, J = 8.2 Hz, 2H), 6.72 (d, J = 8.1 Hz, 2H), 3.69 (t, J = 6.8 Hz, 2H), 2.51 (t, J = 7.8 Hz, 2H), 2.27 (s, 3H), 2.20–2.10 (m, 2H); ^{19}F NMR (376 MHz, $CDCl_3$): δ (ppm) −117.06 (s); ^{13}C NMR (101 MHz, $CDCl_3$): δ (ppm) 161.6, 159.7 (dd, $^1J_{CF}$ = 252.1, $^3J_{CF}$ = 5.8 Hz), 149.5, 131.5, 129.3, 128.0 (t, $^3J_{CF}$ = 10.0 Hz), 121.9, 118.1, 112.3 (dd, $^3J_{CF}$ = 18.4, 5.2 Hz), 50.8, 26.8, 21.4, 20.9; HRMS (ESI-TOF) *m*/*z*: [M + H]$^+$ calcd for $C_{17}H_{17}F_2N_2$ 287.1360; found: 287.1355.

Compound **3c**: 270 mg, 45%, colorless oil. MS (ESI, pos. ion) *m*/*z*: 303.1 ([M + H]$^+$); ^{1}H NMR (400 MHz, $CDCl_3$): δ (ppm) 7.25–7.15 (m, 1H), 6.96 (t, J = 8.4 Hz, 2H), 6.76 (q, J = 8.9 Hz, 4H), 3.76 (s, 3H), 3.68 (t, J = 6.8 Hz, 2H), 2.50 (t, J = 7.7 Hz, 2H), 2.19–2.09 (m, 2H); ^{19}F NMR (376 MHz, $CDCl_3$): δ (ppm) −117.07 (s); ^{13}C NMR (151 MHz, $CDCl_3$): δ (ppm) 161.9, 159.7 (dd, $^1J_{CF}$ = 252.0, $^3J_{CF}$ = 5.6 Hz), 155.2, 145.5, 128.0 (t, $^3J_{CF}$ = 10.0 Hz), 122.8, 114.1, 112.3 (dd, $^3J_{CF}$ = 19.8, 4.0 Hz), 55.6, 50.7, 26.9, 21.4; HRMS (ESI-TOF) *m*/*z*: [M + H]$^+$ calcd for $C_{17}H_{17}F_2N_2O$ 303.1309; found: 303.1337.

Compound **3d**: 201 mg, 13%, yellow oil. MS (ESI, pos. ion) *m*/*z*: 341.2([M + H]$^+$); ^{1}H NMR (400 MHz, $CDCl_3$) δ (ppm) 7.46 (d, J = 8.2 Hz, 2H), 7.28–7.19 (m, 1H), 6.98 (t, J = 8.2 Hz, 2H), 6.88 (d, J = 8.1 Hz, 2H), 3.73 (t, J = 6.8 Hz, 2H), 2.51 (t, J = 7.8 Hz, 2H), 2.23–2.13 (m, 2H); ^{19}F NMR (376 MHz, $CDCl_3$): δ (ppm) −62.09 (s), −117.18 (s); ^{13}C NMR (101 MHz, $CDCl_3$): δ (ppm) 161.6, 159.6 (dd, $^3J_{CF}$ = 252.1, $^3J_{CF}$ = 5.6 Hz), 155.6, 128.4 (t, $^3J_{CF}$ = 10.0 Hz), 125.9 (d, $^3J_{CF}$ = 3.6 Hz), 124.9–123.2 (m), 122.2, 117.6 (t, $^3J_{CF}$ = 16.1 Hz), 112.3 (dd, $^3J_{CF}$ = 18.4, 4.8 Hz), 50.8, 26.9, 21.3; HRMS (ESI-TOF) *m*/*z*: [M + H]$^+$ calcd for $C_{17}H_{14}F_5N_2$ 341.1077; found: 341.1086.

Compound **3e**: 80 mg, 3%, yellow oil. MS (ESI, pos. ion) *m*/*z*: 318.1 ([M + H]$^+$); ^{1}H NMR (400 MHz, $CDCl_3$): δ (ppm) 8.09 (d, J = 8.4 Hz, 2H), 7.32–7.17 (m, 1H), 6.98 (t, J = 8.0 Hz, 2H), 6.87 (d, J = 8.8 Hz, 2H), 3.75 (t, J = 6.9 Hz, 2H), 2.56 (t, J = 7.7 Hz, 2H), 2.26–2.19 (m, 2H); ^{19}F NMR (376 MHz, $CDCl_3$): δ (ppm) −117.30 (s); ^{13}C NMR (151 MHz, $CDCl_3$): δ (ppm) 160.1 (d, $^1J_{CF}$ = 394.9 Hz), 159.4 (dd, $^1J_{CF}$ = 252.8, $^3J_{CF}$ = 4.9 Hz), 142.9, 128.8 (t, $^3J_{CF}$ = 10.0 Hz), 124.9, 122.5, 112.3 (dd, $^3J_{CF}$ = 19.7, 3.8 Hz), 51.0, 27.3, 21.3; HRMS (ESI-TOF) *m*/*z*: [M + H]$^+$ calcd for $C_{16}H_{14}F_2N_3O_2$ 318.1054; found: 318.1045.

Compound **4a**: 133 mg, 30%, colorless oil. MS (ESI, pos. ion) *m*/*z*: 331.1 ([M + H]$^+$); ^{1}H NMR (400 MHz, $CDCl_3$): δ (ppm) 7.29–7.17 (m, 3H), 6.97 (t, J = 8.3 Hz, 3H), 6.83–6.81 (m, 2H), 3.98–3.86 (m, 2H), 3.74 (s, 3H), 3.43–3.35 (m, 1H), 2.81 (ABX, J = 16.7, 8.2, 9.0 Hz, 2H); ^{19}F NMR (376 MHz, $CDCl_3$): δ (ppm) −116.31 (s), −117.41 (s); ^{13}C NMR (151 MHz, $CDCl_3$): δ (ppm) 172.8, 159.6 (dd, $^3J_{CF}$ = 251.7, $^1J_{CF}$ = 5.4 Hz), 158.8, 151.5, 128.9, 128.5 (t, $^3J_{CF}$ = 10.0 Hz), 122.6, 121.9, 117.1 (t, $^3J_{CF}$ = 16.0 Hz), 112.5 (td, $^3J_{CF}$ = 12.2, 2.1 Hz), 52.5, 52.3, 39.3, 29.9; HRMS (ESI-TOF) *m*/*z*: [M + H]$^+$ calcd for $C_{18}H_{17}F_2N_2O_2$ 331.1258; found: 331.1269.

Compound **4b**: 153 mg, 43%, yellow oil. MS (ESI, pos. ion) *m*/*z*: 345.2 ([M + H]$^+$); ^{1}H NMR (400 MHz, $CDCl_3$): δ (ppm) 7.21 (ddd, J = 14.6, 8.3, 6.3 Hz, 1H), 7.03 (d, J = 7.9 Hz, 2H), 6.95 (t, J = 8.8 Hz, 2H), 6.72 (d, J = 8.0 Hz, 2H), 3.95–3.86 (m, 2H), 3.73 (s, 3H), 3.37 (p, J = 8.1 Hz, 1H), 2.81 (ABX, J = 16.7, 8.2, 9.0 Hz, 2H), 2.27 (s, 3H); ^{19}F NMR (376 MHz, $CDCl_3$): δ (ppm) −116.26, −117.41 (s).^{13}C NMR (101 MHz, $CDCl_3$): δ (ppm) 172.9, 159.7 (dd, $^1J_{CF}$ = 251.4, $^3J_{CF}$ = 5.4 Hz), 159.1, 148.8, 131.9, 129.5, 128.5 (t, $^3J_{CF}$ = 10.0 Hz), 121.8, 117.2 (t, $^3J_{CF}$ = 16.0 Hz), 112.3 (dd, $^3J_{CF}$ = 18.5, 11.3 Hz), 52.5, 52.3, 39.3, 29.9, 20.9; HRMS (ESI-TOF) *m*/*z*: [M + H]$^+$ calcd for $C_{19}H_{19}F_2N_2O_2$ 345.1415; found: 345.1424.

Compound **4c**: 167 mg, 40%, pale yellow oil. MS (ESI, pos. ion) *m*/*z*: 361.1 ([M + H]$^+$); ^{1}H NMR (400 MHz, $CDCl_3$): δ (ppm) 7.26–7.19 (m, 1H), 6.97 (t, J = 8.6 Hz, 2H), 6.80–6.73 (m, 4H), 3.96–3.84 (m, 2H), 3.76 (s, 3H), 3.74 (s, 3H), 3.42–3.36 (m, 1H), 2.80 (ABX, J = 16.7, 8.3, 9.0 Hz, 2H); ^{19}F NMR (376 MHz, $CDCl_3$): δ (ppm) −116.31 (s), −117.42 (s); ^{13}C NMR (151 MHz, $CDCl_3$): δ (ppm) 172.9, 159.6 (d, $^1J_{CF}$ = 251.7 Hz), 159.3, 155.4, 144.8, 128.4 (t, $^3J_{CF}$ = 10.0 Hz), 122.7, 117.2 (t, $^3J_{CF}$ = 15.9 Hz), 114.2, 112.3 (td, $^3J_{CF}$ = 19.9, 3.2 Hz), 55.57, 52.53, 52.26, 39.35, 29.92; HRMS (ESI-TOF) *m*/*z*: [M + H]$^+$ calcd for $C_{19}H_{19}F_2N_2O_3$ 361.1364; found: 361.1361.

Compound **4d**: 166 mg, 21%, colorless oil. MS (ESI, pos. ion) *m*/*z*: 399.2 ([M + H]$^+$); ^{1}H NMR (400 MHz, $CDCl_3$): δ (ppm) 7.48

© 2022 The Author(s). Published by the Royal Society of Chemistry

Open Access Article. Published on 09 November 2022. Downloaded on 2/10/2026 6:58:20 PM. This article is licensed under a Creative Commons Attribution-NonCommercial 3.0 Unported Licence.

(d, J = 8.2 Hz, 2H), 7.26 (dt, J = 8.3, 6.3 Hz, 1H), 6.99 (t, J = 8.6 Hz, 2H), 6.90 (d, J = 8.1 Hz, 2H), 3.94 (d, J = 7.7 Hz, 2H), 3.46–3.35 (m, 1H), 2.80 (ABX, J = 16.8, 7.9, 9.0 Hz, 2H); ^{19}F NMR (376 MHz, $CDCl_3$): δ (ppm) −62.20 (s), −116.49 (s), −117.47 (s); ^{13}C NMR (101 MHz, $CDCl_3$): δ (ppm) 172.7, 159.6 (dd, $^1J_{CF}$ = 252.6, $^3J_{CF}$ = 5.3 Hz), 159.1, 154.9, 128.9 (t, $^3J_{CF}$ = 9.9 Hz), 126.2 (d, $^3J_{CF}$ = 3.6 Hz), 122.1, 116.7, 112.4 (dd, $^2J_{CF}$ = 21.8, $^3J_{CF}$ 10.2 Hz), 52.7, 52.5, 39.3, 30.0; HRMS (ESI-TOF) m/z: $[M + H]^+$ calcd for $C_{19}H_{16}F_5N_2O_2$ 399.1132; found: 399.1125.

Compound **4e**: 15 mg, 4%, pale yellow oil. MS (ESI, pos. ion) m/z: 376.0 ($[M + H]^+$); ^{1}H NMR (400 MHz, $CDCl_3$): δ (ppm) 8.13 (d, J = 8.2 Hz, 2H), 7.30–7.23 (m, 1H), 6.98 (t, J = 8.0 Hz, 2H), 6.91 (d, J = 8.7 Hz, 2H), 3.97 (d, J = 7.5 Hz, 2H), 3.76 (s, 3H), 3.48–3.40 (m, 1H), 2.56 (ABX, J = 16.7, 7.6, 8.9 Hz, 2H); ^{19}F NMR (376 MHz, $CDCl_3$): δ (ppm) −116.65 (s), −117.47 (s); ^{13}C NMR (151 MHz, $CDCl_3$): δ (ppm) 172.5, 159.3 (dd, $^1J_{CF}$ = 252.9, $^3J_{CF}$ = 3.6 Hz), 158.9, 158.1, 143.1, 129.1 (t, $^3J_{CF}$ = 9.9 Hz), 124.9, 122.3, 116.3, 112.5–112.1 (m), 52.7, 52.6, 39.1, 30.1; HRMS (ESI-TOF) m/z: $[M + H]^+$ calcd for $C_{18}H_{16}F_2N_3O_4$ 376.1109; found: 376.1108.

4.2.4. General procedure for the synthesis of compounds 4f–4r. A solution of 3-chlorobenzenecarboperoxoic acid (1.30 g, 7.53 mmol) in dichloromethane (20 mL) was added dropwise to a solution of compound **2b** (500 mg, 1.84 mmol) and *N*,*N*-dimethylbenzene-1,4-diamine (505 mg, 3.71 mmol) in dichloromethane (7 mL) below 5 °C. The reaction mixture was stirred at 0 °C for 30 minutes then concentrated *in vacuo* and the resulting solid was dissolved in ethyl acetate (50 mL). The solution was washed with saturated sodium carbonate aqueous solution (50 mL × 2) and brine (20 mL), dried over anhydrous Na_2SO_4 and concentrated *in vacuo*. The residue was purified by a flash column chromatography (EtOAc/PE (v/v) = 1/10 to 1/4) to give compound **4f** (330 mg, 48%) as a pale brown oil. MS (ESI, pos. ion) m/z: 374.0 ($[M + H]^+$); ^{1}H NMR (400 MHz, $CDCl_3$): δ (ppm) 7.25–7.17 (m, 1H), 6.96 (t, J = 8.6 Hz, 2H), 6.70 (dd, J = 23.2, 8.9 Hz, 4H), 3.93–3.84 (m, 2H), 3.73 (s, 3H), 3.41–3.33 (m, 1H), 2.87 (s, 6H), 2.92 (ABX, J = 16.7, 8.4, 9.0 Hz, 2H); ^{19}F NMR (376 MHz, $CDCl_3$): δ (ppm) −116.17 (s), −117.37 (s); ^{13}C NMR (151 MHz, $CDCl_3$): δ (ppm) 172.9, 159.7 (dd, $^1J_{CF}$ = 250.8, 5.3 Hz), 159.0, 147.0, 142.0, 128.3 (t, $^3J_{CF}$ = 10.0 Hz), 122.5, 117.4 (t, $^3J_{CF}$ = 16.0 Hz), 114.0, 112.5–112.1 (m), 52.4, 52.2, 41.5, 39.4, 30.0; HRMS (ESI-TOF) m/z: $[M + H]^+$ calcd for $C_{20}H_{22}F_2N_3O_2$ 374.1680; found: 374.1687.

Compound **4g**: 168 mg, 65%, pale brown oil. MS (ESI, pos. ion) m/z: 349.1 ($[M + H]^+$); ^{1}H NMR (400 MHz, $CDCl_3$): δ (ppm) 7.28–7.19 (m, 1H, Ph–F), 6.97 (t, J = 8.5 Hz, 2H, Ph–F), 6.92 (d, J = 8.7 Hz, 2H, Ph–N=C), 6.79–6.73 (m, 2H, Ph–N=C), 3.92 (d, J = 7.8 Hz, 2H, CH_2N), 3.74 (s, 3H, Me), 3.44–3.32 (m, 1H, CH), 2.79 (ABX, J = 16.7, 8.1, 9.0 Hz, 2H, $CNCH_2$); ^{19}F NMR (376 MHz, $CDCl_3$): δ (ppm) −116.46 (s), −117.47 (s), −122.76 (s); ^{13}C NMR (150 MHz, $CDCl_3$): δ (ppm) 172.8, 160.4 (d, $^3J_{CF}$ = 3.6 Hz), 159.9, 159.5, 158.8, 158.3, 147.6 (d, $^3J_{CF}$ = 2.6 Hz), 128.6 (t, $^3J_{CF}$ = 10.0 Hz), 123.0 (d, $^3J_{CF}$ = 7.9 Hz), 117.0 (t, $^3J_{CF}$ = 16.0 Hz), 115.5, 115.4, 112.5–112.2 (m), 52.6, 52.4, 39.3, 29.9; HRMS (ESI-TOF) m/z: $[M + H]^+$ calcd for $C_{18}H_{16}F_3N_2O_2$ 349.1164; found: 349.1155.

Compound **4h**: 554 mg, 82%, pale brown oil. MS (ESI, pos. ion) m/z: 365.1 ($[M + H]^+$); ^{1}H NMR (400 MHz, $CDCl_3$): δ (ppm) 7.28–7.19 (m, 1H, Ph–F), 7.18 (d, J = 8.6 Hz, 2H, Ph–Cl), 6.97 (t, J = 8.5 Hz, 2H, Ph–F), 6.75 (d, J = 8.6 Hz, 2H, Ph–Cl), 3.92 (d, J = 7.7 Hz, 2H, CH_2N), 3.74 (s, 3H, Me), 3.45–3.33 (m, 1H, CH), 2.79 (ABX, J = 16.7, 8.0, 9.0 Hz, 2H, $CNCH_2$); ^{19}F NMR (376 MHz, $CDCl_3$): δ (ppm) −116.46 (s), −117.46 (s); ^{13}C NMR (150 MHz, $CDCl_3$): δ (ppm) 172.7, 160.4 (d, $^3J_{CF}$ = 5.5 Hz), 159.3, 158.7, 150.2, 128.9, 128.7 (t, $^3J_{CF}$ = 10.0 Hz), 127.8, 123.3, 116.9 (t, $^3J_{CF}$ = 16.0 Hz), 112.6–112.2 (m), 52.6, 52.4, 39.3, 29.9; HRMS (ESI-TOF) m/z: $[M + H]^+$ calcd for $C_{18}H_{16}ClF_2N_2O_2$ 365.0868; found: 365.0851.

Compound **4i**: 700 mg, 91%, pale brown oil. MS (ESI, pos. ion) m/z: 409.0 ($[M + H]^+$); ^{1}H NMR (400 MHz, $CDCl_3$): δ (ppm) 7.33 (d, J = 8.5 Hz, 2H, Ph–Br), 7.29–7.19 (m, 1H, Ph–F), 6.97 (t, J = 8.5 Hz, 2H, Ph–F), 6.70 (d, J = 8.5 Hz, 2H, Ph–Br), 3.92 (d, J = 7.7 Hz, 2H, CH_2N), 3.74 (s, 3H, Me), 3.45–3.33 (m, 1H, CH), 2.79 (ABX, J = 16.7, 8.0, 9.0 Hz, 2H, $CNCH_2$); ^{19}F NMR (376 MHz, $CDCl_3$): δ (ppm) −116.46 (s), −117.46 (s); ^{13}C NMR (150 MHz, $CDCl_3$): δ (ppm) 172.7, 160.4 (d, $^3J_{CF}$ = 5.2 Hz), 159.2, 158.7, 150.7, 131.8, 128.7 (t, $^3J_{CF}$ = 10.0 Hz), 123.8, 116.8 (t, $^3J_{CF}$ = 16.0 Hz), 115.5, 112.6–112.2 (m), 52.6, 52.4, 39.3, 29.9; HRMS (ESI-TOF) m/z: $[M + H]^+$ calcd for $C_{18}H_{16}BrF_2N_2O_2$ 409.0363; found: 409.0345.

Compound **4j**: 433 mg, 52%, pale brown oil. MS (ESI, pos. ion) m/z: 457.0 ($[M + H]^+$); ^{1}H NMR (400 MHz, $CDCl_3$): δ (ppm) 7.51 (d, J = 8.5 Hz, 2H, Ph–I), 7.31–7.18 (m, 1H, Ph–F), 6.97 (t, J = 8.6 Hz, 2H, Ph–F), 6.59 (d, J = 8.5 Hz, 2H, Ph–I), 3.92 (d, J = 7.7 Hz, 2H, CH_2N), 3.74 (s, 3H, Me), 3.45–3.32 (m, 1H, CH), 2.79 (ABX, J = 16.7, 8.0, 9.0 Hz, 2H, $CNCH_2$); ^{19}F NMR (376 MHz, $CDCl_3$): δ (ppm) −116.44 (s), −117.44 (s); ^{13}C NMR (150 MHz, $CDCl_3$): δ (ppm) 172.7, 160.4 (d, $^3J_{CF}$ = 5.4 Hz), 159.1, 158.7 (d, $^3J_{CF}$ = 4.5 Hz), 151.4, 137.8, 128.7 (t, $^3J_{CF}$ = 10.0 Hz), 124.3, 117.4, 116.8 (t, $^3J_{CF}$ = 16.0 Hz), 112.5–112.2 (m), 85.9, 52.6, 52.4, 39.2, 29.9; HRMS (ESI-TOF) m/z: $[M + H]^+$ calcd for $C_{18}H_{16}F_2IN_2O_2$ 457.0225; found: 457.0212.

Compound **4k**: 96 mg, 28%, yellow oil. MS (ESI, pos. ion) m/z: 356.2 ($[M + H]^+$); ^{1}H NMR (400 MHz, $CDCl_3$): δ (ppm) 7.52 (d, J = 7.7 Hz, 2H, Ph–CN), 7.32–7.21 (m, 1H, Ph–F), 6.99 (t, J = 8.4 Hz, 2H, Ph–F), 6.88 (d, J = 8.0 Hz, 2H, Ph–CN), 3.95 (d, J = 7.6 Hz, 2H, CH_2N), 3.76 (s, 3H, Me), 3.48–3.36 (m, 1H, CH), 2.81 (ABX, J = 16.8, 7.6, 8.8 Hz, 2H, $CNCH_2$); ^{19}F NMR (376 MHz, $CDCl_3$): δ (ppm) −116.61 (s), −117.48 (s); ^{13}C NMR (100 MHz, $CDCl_3$): δ (ppm) 172.5, 160.7, 159.0, 158.2, 156.0, 133.2, 129.0 (t, $^3J_{CF}$ = 10.0 Hz), 122.8, 119.7, 112.4 (dd, $^3J_{CF}$ = 17.0, 10.9 Hz), 105.7, 52.7, 52.5, 39.2, 30.0; HRMS (ESI-TOF) m/z: $[M + H]^+$ calcd for $C_{19}H_{16}F_2N_3O_2$ 356.1211; found: 356.1204.

Compound **4l**: 123 mg, 62%, yellow oil. MS (ESI, pos. ion) m/z: 389.0 ($[M + H]^+$); ^{1}H NMR (400 MHz, $CDCl_3$): δ (ppm) 7.93 (d, J = 8.3 Hz, 2H, Ph–CO_2Me), 7.29–7.21 (m, 1H, Ph–F), 6.98 (t, J = 8.7 Hz, 2H, Ph–F), 6.87 (d, J = 8.3 Hz, 2H, Ph–CO_2Me), 3.95 (d, J = 7.7 Hz, 2H, CH_2N), 3.88 (s, 3H, Ph–CO_2Me), 3.75 (s, 3H, Me), 3.47–3.36 (m, 1H, CH), 2.82 (ABX, J = 16.8, 7.9, 9.0 Hz, 2H, $CNCH_2$); ^{19}F NMR (376 MHz, $CDCl_3$): δ (ppm) −116.49 (s), −117.46 (s); ^{13}C NMR (100 MHz, $CDCl_3$): δ (ppm) 172.7, 167.3, 160.9, 158.8, 158.3, 156.2, 130.8, 128.9 (t, $^3J_{CF}$ = 10.0 Hz), 124.5, 121.9, 116.7, 112.6–112.1 (m), 52.6, 52.5, 51.9, 39.3, 30.0; HRMS (ESI-TOF) m/z: $[M + H]^+$ calcd for $C_{20}H_{19}F_2N_2O_4$ 389.1313; found: 389.1307.

Open Access Article. Published on 09 November 2022. Downloaded on 2/10/2026 6:58:20 PM. This article is licensed under a Creative Commons Attribution-NonCommercial 3.0 Unported Licence.

Compound **4m**: 150 mg, 70%, yellow oil. MS (ESI, pos. ion) *m*/*z*: 388.5 ([M + H]$^+$); ^{1}H NMR (400 MHz, $CDCl_3$): δ (ppm) 7.33 (d, J = 8.6 Hz, 2H, Ph–NH), 7.25–7.18 (m, 1H, Ph–F), 7.17 (br. s, 1H, NH), 6.96 (t, J = 8.7 Hz, 2H, Ph–F), 6.77 (d, J = 8.5 Hz, 2H, Ph–NH), 3.96–3.85 (m, 2H, CH_2N), 3.74 (s, 3H, Me), 2.80 (ABX, J = 16.8, 8.0, 9.0 Hz, 2H, $CNCH_2$), 2.13 (s, 3H, COMe); ^{19}F NMR (376 MHz, $CDCl_3$): δ (ppm) −116.34 (s), −117.40 (s); ^{13}C NMR (100 MHz, $CDCl_3$): δ (ppm) 172.8, 168.4, 160.8 (d, $^3J_{CF}$ = 5.3 Hz), 159.6, 158.3, 147.6, 133.3, 128.7 (t, $^3J_{CF}$ = 9.9 Hz), 122.2, 120.9, 117.0 (t, $^3J_{CF}$ = 16.0 Hz), 112.3 (dd, $^3J_{CF}$ = 18.5, 9.8 Hz), 52.6, 52.4, 39.3, 30.1, 24.4; HRMS (ESI-TOF) *m*/*z*: [M + H]$^+$ calcd for $C_{20}H_{20}F_2N_3O_3$ 388.1473; found: 388.1469.

Compound **4n**: 150 mg, 22%, pale yellow oil. MS (ESI, pos. ion) *m*/*z*: 373.0 ([M + H]$^+$); ^{1}H NMR (400 MHz, $CDCl_3$): δ (ppm) 7.88 (d, J = 8.1 Hz, 2H, Ph–COMe), 7.29–7.22 (m, 1H, Ph–F), 6.97 (t, J = 8.6 Hz, 2H, Ph–F), 6.89 (d, J = 8.1 Hz, 2H, Ph–COMe), 3.96 (d, J = 7.7 Hz, 2H, CH_2N), 3.75 (s, 3H, Me), 3.46–3.38 (m, 1H, CH), 2.77 (ABX, J = 16.8, 7.9, 9.0 Hz, 2H, $CNCH_2$), 2.55 (s, 3H, COMe); ^{19}F NMR (376 MHz, $CDCl_3$): δ (ppm) −116.47 (s), −117.42 (s); ^{13}C NMR (100 MHz, $CDCl_3$): δ (ppm) 197.3, 172.5, 160.7, 158.7, 158.1, 156.3, 131.9, 129.6, 128.8 (t, $^3J_{CF}$ = 9.9 Hz), 121.9, 116.6 (t, $^3J_{CF}$ = 15.8 Hz), 112.2 (dd, $^3J_{CF}$ = 19.7, 7.8 Hz), 52.5, 52.4, 39.1, 29.9, 26.3; HRMS (ESI-TOF) *m*/*z*: [M + H]$^+$ calcd for $C_{20}H_{19}F_2N_2O_3$ 373.1364; found: 373.1356.

Compound **4o**: 150 mg, 57%, yellow oil. MS (ESI, pos. ion) *m*/*z*: 356.9 ([M + H]$^+$); ^{1}H NMR (400 MHz, $CDCl_3$): δ (ppm) 7.29 (d, J = 8.1 Hz, 2H, Ph–CH=CH_2), 7.25–7.19 (m, 1H, Ph–F), 6.98 (t, J = 8.7 Hz, 2H, Ph–F), 6.78 (d, J = 8.2 Hz, 2H, Ph–CH=CH_2), 6.66 (dd, J = 17.6, 10.9 Hz, 1H, Ph–CH=CH_2), 5.63 (d, J = 17.6 Hz, 1H, Ph–CH=CH_2), 5.11 (d, J = 10.9 Hz, 1H, Ph–CH=CH_2), 3.97–3.87 (m, 2H, CH_2N), 3.75 (s, 3H, Me), 3.46–3.38 (m, 1H, CH), 2.82 (ABX, J = 16.7, 8.1, 9.0 Hz, 2H, $CNCH_2$); ^{19}F NMR (376 MHz, $CDCl_3$): δ (ppm) −116.33 (s), −117.41 (s); ^{13}C NMR (100 MHz, $CDCl_3$): δ (ppm) 172.8, 160.9 (d, $^3J_{CF}$ = 5.5 Hz), 158.8, 158.4 (d, $^3J_{CF}$ = 5.4 Hz), 151.4, 136.9, 132.2), 128.5 (t, $^3J_{CF}$ = 10.0 Hz), 126.9, 122.1, 117.1 (t, $^3J_{CF}$ = 16.0 Hz), 112.4 (dd, $^3J_{CF}$ = 16.9, 12.8 Hz), 111.7, 52.5, 52.3, 39.4, 30.0; HRMS (ESI-TOF) *m*/*z*: [M + H]$^+$ calcd for $C_{20}H_{19}F_2N_2O_2$ 357.1415; found: 357.1438.

Compound **4p**: 126 mg, 43%, yellow oil. MS (ESI, pos. ion) *m*/*z*: 375.3 ([M + H]$^+$); ^{1}H NMR (400 MHz, $CDCl_3$): δ (ppm) 7.21 (td, J = 8.4, 4.2 Hz,1H, Ph–F), 6.96 (t, J = 8.6 Hz, 2H, Ph–F), 6.75 (q, J = 8.9 Hz, 4H, Ph–OCH_2CH_3), 3.97 (q, J = 7.0 Hz, 2H, OCH_2), 3.93–3.86 (m, 2H, CH_2N), 3.73 (s, 3H, OMe), 3.43–3.31 (m, 1H, CH), 2.80 (ABX, J = 16.7, 8.2, 9.0 Hz, 2H, $CNCH_2$), 1.38 (t, J = 7.0 Hz, 3H, OCH_2CH_3); ^{19}F NMR (376 MHz, $CDCl_3$): δ (ppm) −116.33 (s), −117.42 (s); ^{13}C NMR (150 MHz, $CDCl_3$): δ (ppm) 172.9, 160.9 (d, $^3J_{CF}$ = 5.5 Hz), 159.1, 158.4, 154.8, 144.8, 128.4 (t, $^3J_{CF}$ = 10.0 Hz), 122.6, 117.3 (t, $^3J_{CF}$ = 16.0 Hz), 114.9, 112.5–112.1 (m), 63.8, 52.5, 52.2, 39.4, 29.9, 15.1; HRMS (ESI-TOF) *m*/*z*: [M + H]$^+$ calcd for $C_{20}H_{21}F_2N_2O_3$ 375.1520; found:375.1540.

Compound **4q**: 180 mg, 81%, pale yellow oil. MS (ESI, pos. ion) *m*/*z*: 402.5 ([M + H]$^+$); ^{1}H NMR (400 MHz, $CDCl_3$): δ (ppm) 7.32 (d, J = 8.2 Hz, 2H, Ph–CO), 7.29–7.18 (m, 1H, Ph–F), 6.98 (t, J = 8.6 Hz, 2H, Ph–F), 6.84 (d, J = 8.1 Hz, 2H, Ph–CO), 3.99–3.87 (m, 2H, CH_2N), 3.75 (s, 3H, Me), 3.47–3.34 (m, 1H, CH), 3.16–2.92 (m, 6H, NMe_2), 2.80 (ABX, J = 16.8, 7.9, 9.0 Hz, 2H, $CNCH_2$); ^{19}F NMR (376 MHz, $CDCl_3$): δ (ppm) −116.40 (s), −117.42 (s); ^{13}C NMR (100 MHz, $CDCl_3$): δ (ppm) 172.6, 172.0, 171.1 (d, $^3J_{CF}$ = 7.4 Hz), 160.7 (d, $^3J_{CF}$ = 5.4 Hz), 158.9, 158.2 (d, $^3J_{CF}$ = 5.4 Hz), 152.9, 130.3, 128.6 (t, $^3J_{CF}$ = 10.0 Hz), 128.2, 121.6, 116.8 (t, $^3J_{CF}$ = 16.0 Hz), 112.2 (ddd, $^2J_{CF}$ = 20.2, $^3J_{CF}$ = 11.2, 3.1 Hz), 60.4, 52.5, 52.3, 39.2, 29.9, 21.0, 14.2; HRMS (ESI-TOF) *m*/*z*: [M + H]$^+$ calcd for $C_{21}H_{22}F_2N_3O_3$ 402.1629; found: 402.1620.

4.2.5. General procedure for the synthesis of compounds 5b and 5e. To a solution of 2,6-difluoro-4-methoxyaniline (200 mg, 1.26 mmol) and Et_3N (191 mg, 1.89 mmol) in CH_2Cl_2 (2 mL) was added 4-chlorobutanoyl chloride (355 mg, 2.51 mmol) dropwise at 0 °C. The reaction mixture was stirred at 25 °C for 3 h, quenched with water (10 mL) and extracted with CH_2Cl_2 (10 mL × 3). The combined organic phases were washed with brine (10 mL), dried over anhydrous Na_2SO_4 and concentrated *in vacuo*. The residue was purified by a flash column chromatography (EtOAc/PE (v/v) = 1/10 to 3/7) to give 4-chloro-*N*-(2,6-difluoro-4-methoxyphenyl)butanamide (**5bc**) (300 mg, 91%) as colorless oil; MS (ESI, pos. ion) *m*/*z*: 264.3 ([M + H]$^+$); ^{1}H NMR (400 MHz, $CDCl_3$): δ (ppm) 7.75 (brs, 1H), 6.44 (d, J = 9.4 Hz, 2H), 3.73 (s, 3H), 3.60 (t, J = 6.2 Hz, 2H), 2.53 (t, J = 7.1 Hz, 2H), 2.19–2.08 (m, 2H); ^{19}F NMR (376 MHz, $CDCl_3$): δ (ppm) −117.68 (s); ^{13}C NMR (151 MHz, $CDCl_3$): δ (ppm) 171.6 (d, $^3J_{CF}$ = 12.1 Hz), 158.7 (dd, $^1J_{CF}$ = 248.5, $^3J_{CF}$ = 7.8 Hz), 159.4 (t, $^3J_{CF}$ = 13.3 Hz), 106.4 (t, $^3J_{CF}$ = 17.2 Hz), 98.1 (dd, $^2J_{CF}$ = 23.1, $^3J_{CF}$ = 4.0 Hz), 55.9, 44.3, 32.7, 28.2; HRMS (ESI-TOF) *m*/*z*: [M + H]$^+$ calcd for $C_{11}H_{13}ClF_2NO_2$ 264.0603; found: 264.0598.

To a solution of compound **5bc** (300 mg, 1.14 mmol) in DMF (2 mL) was added DBU (260 mg, 1.71 mmol) at room temperature. The reaction mixture was heated at 100 °C and stirred overnight. The reaction was quenched with water (10 mL) and extracted with CH_2Cl_2 (10 mL × 3). The combined organic phases were washed with brine (10 mL), dried over anhydrous Na_2SO_4 and concentrated *in vacuo*. The residue was purified by a flash column chromatography (EtOAc/PE (v/v) = 1/10 to 1/5) to give compound **5b** (220 mg, 85%) as pale yellow oil; MS (ESI, pos. ion) *m*/*z*: 228.1 ([M + H]$^+$); ^{1}H NMR (400 MHz, $CDCl_3$): δ (ppm) 6.51 (d, J = 9.5 Hz, 2H), 3.77 (s, 3H), 3.70 (t, J = 7.0 Hz, 2H), 2.54 (t, J = 8.1 Hz, 2H), 2.31–2.14 (m, 2H); ^{19}F NMR (376 MHz, $CDCl_3$): δ (ppm) −117.42 (s); ^{13}C NMR (151 MHz, $CDCl_3$): δ (ppm) 175.3, 159.6 (dd, $^1J_{CF}$ = 250.2, $^3J_{CF}$ = 8.2 Hz), 160.2 (t, $^3J_{CF}$ = 13.5 Hz), 108.3 (t, $^3J_{CF}$ = 17.2 Hz), 98.7 (dd, $^2J_{CF}$ = 23.0, $^3J_{CF}$ = 4.3 Hz), 56.1, 49.6, 30.4, 19.2; HRMS (ESI-TOF) *m*/*z*: [M + H]$^+$ calcd for $C_{11}H_{12}F_2NO_2$ 228.0836; found: 228.0831.

Compound **5ec**: 322 mg, 88%, pale yellow oil. MS (ESI, pos. ion) *m*/*z*: 292.0 ([M + H]$^+$).^{1}H NMR (400 MHz, $CDCl_3$): δ (ppm) 7.60 (d, J = 8.0 Hz, 2H), 7.24 (brs, 1H), 3.92 (s, 3H), 3.66 (t, J = 6.1 Hz, 2H), 2.64 (t, J = 7.0 Hz, 2H), 2.25–2.15 (m, 2H); ^{19}F NMR (376 MHz, $CDCl_3$): δ (ppm) −116.47 (s); ^{13}C NMR (151 MHz, $CDCl_3$): δ (ppm) 170.4, 164.7, 157.1 (dd, $^1J_{CF}$ = 251.8, $^3J_{CF}$ = 4.7 Hz), 129.7, 118.3 (t, $^3J_{CF}$ = 16.5 Hz), 113.2 (dd, $^2J_{CF}$ = 21.6, $^3J_{CF}$ = 4.3 Hz), 52.9, 44.3, 27.9; HRMS (ESI-TOF) *m*/*z*: [M + H]$^+$ calcd for $C_{12}H_{13}ClF_2NO_3$ 292.0552, found: 292.0548.

Compound **5e**: 133 mg, 82%, pale yellow oil. MS (ESI, pos. ion) *m*/*z*: 256.3 [M + H]$^+$.^{1}H NMR (400 MHz, $CDCl_3$): δ (ppm) 7.63 (d, J = 8.2 Hz, 2H), 3.92 (s, 3H), 3.79 (t, J = 7.0 Hz, 2H), 2.57 (t, J = 8.1 Hz, 2H), 2.28 (m, 2H); ^{19}F NMR (376 MHz, $CDCl_3$): δ (ppm) −115.34 (s); ^{13}C NMR (101 MHz, $CDCl_3$): δ (ppm) 174.6, 164.6 (t,

© 2022 The Author(s). Published by the Royal Society of Chemistry

Open Access Article. Published on 09 November 2022. Downloaded on 2/10/2026 6:58:20 PM.
This article is licensed under a Creative Commons Attribution-NonCommercial 3.0 Unported Licence.

$^3J_{CF}$ = 3.2 Hz), 159.8 (d, $^3J_{CF}$ = 5.3 Hz), 157.3 (d, $^3J_{CF}$ = 5.4 Hz), 130.9 (t, $^3J_{CF}$ = 9.1 Hz), 120.1 (t, $^3J_{CF}$ = 16.5 Hz), 113.5 (m), 52.9, 49.3, 30.4, 19.6; HRMS (ESI-TOF) *m*/*z*: [M + H]$^+$ calcd for $C_{12}H_{12}F_2NO_3$ 256.0785, found: 256.0785.

4.2.6. General procedure for the synthesis of compounds 5c, 5d and 5i. To a solution of 2,6-difluoro-4-(trifluoromethyl) aniline (200 mg, 1.01 mmol) and NaH (50 mg, 60% dispersion in mineral oil) in DMF (2 mL) was added 4-chlorobutanoyl chloride (143 mg, 1.01 mmol) at 0 °C. The reaction mixture was warmed to room temperature and stirred overnight. The reaction was quenched with water (10 mL) and extracted with CH_2Cl_2 (10 mL × 3). The combined organic phases were washed with brine (10 mL), dried over anhydrous Na_2SO_4 and concentrated *in vacuo*. The residue was purified by a flash column chromatography (EtOAc/PE (v/v) = 1/10 to 1/1) to give compound **5c** (150 mg, 56%) as pale yellow oil; MS (ESI, pos. ion) *m*/*z*: 266.1 [M + H]$^+$; ^{1}H NMR (400 MHz, $CDCl_3$): δ (ppm) 7.27 (d, J = 7.0 Hz, 2H), 3.79 (t, J = 7.0 Hz, 2H), 2.59 (t, J = 8.1 Hz, 2H), 2.35–2.24 (m, 2H); ^{19}F NMR (376 MHz, $CDCl_3$): δ (ppm) −63.66 (s), −113.36 (s); ^{13}C NMR (101 MHz, $CDCl_3$): δ (ppm) 174.6, 159.6 (d, $^3J_{CF}$ = 5.6 Hz), 157.9 (d, $^3J_{CF}$ = 5.6 Hz), 131.0–131.3 (m), 123.9 (t, $^3J_{CF}$ = 2.9 Hz), 122.1 (t, $^3J_{CF}$ = 2.9 Hz), 119.2 (t, $^3J_{CF}$ = 16.0 Hz), 110.1–109.8 (m), 49.1, 30.2, 19.5; HRMS (ESI-TOF) *m*/*z*: [M + H]$^+$ calcd for $C_{11}H_9F_5NO$ 266.0604, found: 266.0591.

Compound **5d**: 175 mg, 13%, yellow oil. MS (ESI, pos. ion) *m*/*z*: 243.1 ([M + H]$^+$); ^{1}H NMR (400 MHz, $CDCl_3$): δ (ppm) 7.94–7.86 (m, 2H, Ph), 3.83 (t, J = 7.0 Hz, 2H, CH_2N), 2.60 (t, J = 8.1 Hz, 2H, $COCH_2$), 2.38–2.27 (m, 2H, CH_2); ^{19}F NMR (376 MHz, $CDCl_3$): δ (ppm) −110.99 (s); ^{13}C NMR (101 MHz, $CDCl_3$): δ (ppm) 174.5, 159.6 (d, $^3J_{CF}$ = 5.9 Hz), 157.0 (d, $^3J_{CF}$ = 5.9 Hz), 146.7 (t, $^3J_{CF}$ = 10.4 Hz), 122.4 (t, $^3J_{CF}$ = 16.3 Hz), 108.8–108.3 (m), 49.1 (t, $^3J_{CF}$ = 2.1 Hz), 30.3, 19.7; HRMS (ESI-TOF) *m*/*z*: [M + H]$^+$ calcd for $C_{10}H_9F_2N_2O_3$ 243.0581, found: 243.0572.

Compound **5i**: 66 mg, 62%, yellow oil. MS (ESI, pos. ion) *m*/*z*: 216.1 ([M + H]$^+$); ^{1}H NMR (400 MHz, $CDCl_3$): δ (ppm) 6.80–6.72 (m, 2H), 3.72 (t, J = 7.0 Hz, 2H), 2.56 (t, J = 8.1 Hz, 2H), 2.33–2.17 (m, 2H); ^{19}F NMR (376 MHz, $CDCl_3$): δ (ppm) −108.04 (t, J = 5.6 Hz), −114.61 (d, J = 7.1 Hz); ^{13}C NMR (151 MHz, $CDCl_3$): δ (ppm) 175.0, 162.5 (t, $^3J_{CF}$ = 14.9 Hz), 160.8 (t, $^3J_{CF}$ = 14.9 Hz), 159.3 (ddd, $^1J_{CF}$ = 253.3, $^3J_{CF}$ = 15.3, 7.7 Hz), 112.4 (td, $^3J_{CF}$ = 16.8, 5.0 Hz), 101.5–100.5 (m), 49.4, 30.3, 19.3; HRMS (ESI-TOF) *m*/*z*: [M + H]$^+$ calcd for $C_{10}H_9F_3NO$ 216.0636, found: 216.0631.

Compound **5f**: To a solution of compound **5d** (500 mg, 2.0 mmol) in MeOH (10 mL) was added Pd/C (50 mg, 10%) and charged with H_2. The reaction mixture was heated to 60 °C and stirred for 5 h, then cooled to room temperature. The mixture was filtered and the filter was concentrated *in vacuo*. The residue was purified by a flash column chromatography (EtOAc/hexanes (v/v) = 1/10 to 2/3) to give compound **5f** (360 mg, 80%) as pale yellow oil; MS (ESI, pos. ion) *m*/*z*: 213.1 ([M + H]$^+$); ^{1}H NMR (400 MHz, $CDCl_3$): δ (ppm) 6.27–6.08 (m, 2H), 4.22 (brs, 2H), 3.66 (t, J = 7.0 Hz, 2H), 2.52 (t, J = 8.1 Hz, 2H), 2.33–2.08 (m, 2H); ^{19}F NMR (376 MHz, $CDCl_3$): δ (ppm) −119.53 (s); ^{13}C NMR (101 MHz, $CDCl_3$): δ (ppm) 175.5, 159.8 (dd, $^1J_{CF}$ = 248.1, $^3J_{CF}$ = 8.0 Hz), 148.3 (t, $^3J_{CF}$ = 13.4 Hz), 105.0 (t, $^3J_{CF}$ = 17.3 Hz), 98.4–98.0 (m), 49.9, 30.5, 19.1; HRMS (ESI-TOF) *m*/*z*: [M + H]$^+$ calcd for $C_{10}H_{11}F_2N_2O$ 213.0839, found: 213.0840.

Compound **5g** and Compound **5h**: To a solution of compound **5f** (246 mg, 1.16 mmol), sulfuric acid (1.5 mL) and formaldehyde (261 mg, 3.48 mmol, 40% in water) in methanol (10 mL) was added $NaBH_4$ (226 mg, 5.79 mmol) at 0 °C. The reaction mixture was warmed to room temperature and stirred overnight. The solvent was evaporated and the residue was dissolved with EtOAc (100 mL). The organic phase was washed with brine (10 mL), dried over anhydrous Na_2SO_4 and concentrated *in vacuo*. The residue was purified by a flash column chromatography (EtOAc/PE (v/v) = 1/10 to 1/1) to give compound **5g** (31 mg, 12%) as pale yellow oil and compound **5h** (66 mg, 24%) as pale yellow oil.

Compound **5g**: MS (ESI, pos. ion) *m*/*z*: 227.1 ([M + H]$^+$); ^{1}H NMR (400 MHz, $CDCl_3$): δ (ppm) 6.16–6.02 (m, 2H), 4.39 (brs, 1H), 3.66 (t, J = 7.0 Hz, 2H), 2.75 (s, 3H), 2.53 (t, J = 8.1 Hz, 2H), 2.28–2.12 (m, 2H); ^{19}F NMR (376 MHz, $CDCl_3$): δ (ppm) −119.85 (s); ^{13}C NMR (151 MHz, $CDCl_3$): δ (ppm) 175.5, 159.9 (dd, $^1J_{CF}$ = 247.3, $^3J_{CF}$ = 8.4 Hz), 150.4 (t, $^3J_{CF}$ = 12.9 Hz), 103.7 (t, $^3J_{CF}$ = 17.5 Hz), 95.4 (d, $^2J_{CF}$ = 26.3 Hz), 50.0, 30.5 (d, $^3J_{CF}$ = 3.6 Hz), 19.1; HRMS (ESI-TOF) *m*/*z*: [M + H]$^+$ calcd for $C_{11}H_{13}F_2N_2O$ 227.0996, found: 227.0995.

Compound **5h**: MS (ESI, pos. ion) *m*/*z*: 241.2 ([M + H]$^+$); ^{1}H NMR (400 MHz, $CDCl_3$): δ (ppm) 6.29–6.11 (m, 2H), 3.67 (t, J = 7.0 Hz, 2H), 2.92 (s, 6H), 2.53 (t, J = 8.1 Hz, 2H), 2.28–2.10 (m, 2H); ^{19}F NMR (376 MHz, $CDCl_3$): δ (ppm) −119.45 (s); ^{13}C NMR (151 MHz, $CDCl_3$): δ (ppm) 175.4, 159.8 (dd, $^1J_{CF}$ = 246.5, $^3J_{CF}$ = 8.8 Hz), 150.9 (t, $^3J_{CF}$ = 13.1 Hz), 103.2 (t, $^3J_{CF}$ = 17.3 Hz), 95.8–95.0 (m), 49.9, 40.3, 30.5, 19.1; HRMS (ESI-TOF) *m*/*z*: [M + H]$^+$ calcd for $C_{12}H_{15}F_2N_2O$ 241.1152, found: 241.1168.

4.2.7. General procedure for the synthesis of compounds 6a–6w. A mixture of 4-substituted-2,6-difluoroaniline (10 mmol) and 2-methylenesuccinic acid (1.30 g, 10 mmol) was heated at 180 °C for 7 h in a sealed tube. The reaction vessel was then cooled to room temperature. The crude product (brown oil) was dissolved in MeOH (50 mL) and concentrated sulfuric acid (0.5 mL) was added. The reaction mixture was refluxed for 4 h and then concentrated *in vacuo*. The residue was purified by a flash column chromatography (EtOAc/hexanes (v/v) = 1/10 to 1/2) to give compound **6**.

Compound **6a**: 368 mg, 43%, pale yellow oil. MS (ESI, pos. ion) *m*/*z*: 270.3 ([M + H]$^+$); ^{1}H NMR (400 MHz, $CDCl_3$): δ (ppm) 6.78 (d, J = 9.3 Hz, 2H), 3.93 (m, 2H), 3.77 (s, 3H), 3.47 (m, 1H), 2.85 (ABX, J = 17.2, 7.8, 9.6 Hz, 2H), 2.34 (s, 3H); ^{19}F NMR (376 MHz, $CDCl_3$): δ (ppm) −118.56 (s), −119.35 (s); ^{13}C NMR (101 MHz, $CDCl_3$): δ (ppm) 172.7, 172.3, 158.6 (dd, $^1J_{CF}$ = 251.9, $^3J_{CF}$ = 5.8 Hz), 140.8 (t, $^3J_{CF}$ = 9.5 Hz), 112.8 (dd, $^3J_{CF}$ = 19.9, 2.7 Hz), 112.0 (t, $^3J_{CF}$ = 16.7 Hz), 52.7, 50.9, 37.4, 33.4, 21.5; HRMS (ESI-TOF) *m*/*z*: [M + H]$^+$ calcd for $C_{13}H_{14}F_2NO_3$ 270.0942; found: 270.0936.

Compound **6b**: 657 mg, 75%, pale yellow oil. MS (ESI, pos. ion) *m*/*z*: 286.0 ([M + H]$^+$); ^{1}H NMR (400 MHz, $CDCl_3$): δ (ppm) 6.52 (m, 2H), 3.93 (m, 2H), 3.77 (s, 3H), 3.47 (m, 1H), 2.85 (ABX, J = 17.2, 7.8, 9.6 Hz, 2H), 2.34 (s, 3H); ^{19}F NMR (376 MHz, $CDCl_3$): δ (ppm) −116.75 (s), −117.60 (s); ^{13}C NMR (101 MHz, $CDCl_3$): δ (ppm) 172.8, 172.4, 159.6 (dd, $^1J_{CF}$ = 250.7, $^3J_{CF}$ = 8.0 Hz),

Open Access Article. Published on 09 November 2022. Downloaded on 2/10/2026 6:58:20 PM.
This article is licensed under a Creative Commons Attribution-NonCommercial 3.0 Unported Licence.

160.5 (t, $^3J_{CF}$ = 13.5 Hz), 107.6 (t, $^3J_{CF}$ = 17.1 Hz), 98.7 (dd, $^2J_{CF}$ = 23.9, $^3J_{CF}$ = 3.2 Hz), 56.1, 52.6, 51.1, 37, 33.4; HRMS (ESI-TOF) *m*/*z*: [M + H]$^+$ calcd for $C_{13}H_{14}F_2NO_4$ 286.0891; found: 286.0859.

Compound **6c**: 365 mg, 54%, pale yellow oil. MS (ESI, pos. ion) *m*/*z*: 314.0 ([M + H]$^+$); ^{1}H NMR (600 MHz, $CDCl_3$): δ (ppm) 7.28 (d, *J* = 8.2 Hz, 2H), 4.02 (dd, *J* = 9.6, 6.6 Hz, 1H), 3.97 (t, *J* = 9.1 Hz, 1H), 3.79 (s, 3H), 3.51 (dt, *J* = 16.1, 8.0 Hz, 1H), 2.88 (ABX, *J* = 17.5, 7.6, 9.6 Hz, 2H); ^{19}F NMR (376 MHz, $CDCl_3$): δ (ppm) −63.69 (s), −112.71 (s), −113.42 (s); ^{13}C NMR (151 MHz, $CDCl_3$): δ (ppm) 172.5, 172.0, 158.8 (dd, $^1J_{CF}$ = 255.9, $^3J_{CF}$ = 5.2 Hz), 131.9–131.8 (m), 131.7–131.4 (m), 123.4, 121.6, 118.6–118.1 (m), 110.2 (d, $^2J_{CF}$ = 23.5 Hz), 52.9, 50.6, 37.5, 33.3; HRMS (ESI-TOF) *m*/*z*: [M + H]$^+$ calcd for $C_{13}H_{11}F_5NO_3$ 314.0840; found: 314.0795.

Compound **6e**: 429 mg, 43%, pale yellow oil. MS (ESI, pos. ion) *m*/*z*: 314.0 ([M + H]$^+$); ^{1}H NMR (400 MHz, $CDCl_3$): δ (ppm) 7.66 (d, *J* = 8.6 Hz, 2H), 4.05 (m, 2H), 3.93 (s, 3H), 3.79 (s, 3H), 3.53 (m, 1H), 2.96 (m, 2H); ^{19}F NMR (376 MHz, $CDCl_3$): δ (ppm) −114.76 (s), −115.37 (s); ^{13}C NMR (101 MHz, $CDCl_3$): δ (ppm) 173.8, 172.4, 164.5 (t, $^3J_{CF}$ = 3.0 Hz), 158.5 (dd, $^1J_{CF}$ = 254.3, $^3J_{CF}$ = 5.1 Hz), 131.9 (t, $^3J_{CF}$ = 9.2 Hz), 118.5 (t, $^3J_{CF}$ = 16.4 Hz), 113.6 (dd, $^2J_{CF}$ = 22.1, $^3J_{CF}$ = 3.3 Hz), 53.0 (d, $^3J_{CF}$ = 13.1 Hz), 51.2, 37.4, 33.4; HRMS (ESI-TOF) *m*/*z*: [M + H]$^+$ calcd for $C_{14}H_{14}F_2NO_5$ 314.0840; found: 314.0795.

Compound **6f**: the method as compound **5f**. 390 mg, 93%, yellow oil. MS (ESI, pos. ion) *m*/*z*: 271.3 ([M + H]$^+$); ^{1}H NMR (400 MHz, $CDCl_3$): δ (ppm) 6.18 (d, *J* = 10.2 Hz, 2H), 4.04 (brs, 2H), 3.92–3.80 (m, 2H), 3.77 (s, 3H), 3.50–3.34 (m, 1H), 2.82 (ABX, *J* = 17.2, 7.8, 9.7 Hz, 2H); ^{19}F NMR (376 MHz, $CDCl_3$): δ (ppm) −118.89 (s), −119.70 (s); ^{13}C NMR (101 MHz, $CDCl_3$): δ (ppm) 172.9 (s), 172.7 (s), 159.8 (dd, $^1J_{CF}$ = 248.6, $^3J_{CF}$ = 7.7 Hz), 148.5 (t, $^3J_{CF}$ = 13.5 Hz), 104.3 (t, $^3J_{CF}$ = 16.3 Hz), 98.2 (d, $^2J_{CF}$ = 23.8 Hz), 52.6, 51.34, 37.2, 33.; HRMS (ESI-TOF) *m*/*z*: [M + H]$^+$ calcd for $C_{12}H_{13}F_2N_2O3$ 271.0894, found: 271.0809.

Compound **6g**: the method as compound **5g**. 36 mg, 8%, yellow oil. MS (ESI, pos. ion) *m*/*z*: 285.0 ([M + H]$^+$); ^{1}H NMR (400 MHz, $CDCl_3$): δ (ppm) 6.08 (d, *J* = 10.9 Hz, 2H), 4.33 (d, *J* = 4.3 Hz, 1H), 3.86 (p, *J* = 9.6 Hz, 2H), 3.76 (s, 3H), 3.49–3.36 (m, 1H), 2.83 (ABX, *J* = 17.2, 7.9, 9.7 Hz, 2H), 2.74 (d, *J* = 5.0 Hz, 3H); ^{19}F NMR (376 MHz, $CDCl_3$): δ (ppm) −119.31 (s), −120.0988 (s); ^{13}C NMR (151 MHz, $CDCl_3$): δ (ppm) 172.9, 172.9, 159.9 (dd, $^1J_{CF}$ = 247.6, $^3J_{CF}$ = 8.2 Hz), 150.7 (t, $^3J_{CF}$ = 13.5 Hz), 102.6 (t, $^3J_{CF}$ = 17.5 Hz), 95.3 (dd, $^2J_{CF}$ = 23.5, $^3J_{CF}$ = 7.5 Hz), 52.6, 51.4, 37.1, 33.4, 30.4; HRMS (ESI-TOF) *m*/*z*: [M + H]$^+$ calcd for $C_{13}H_{15}F_2N_2O_3$ 285.1051, found: 285.1050.

Compound **6h**: the method as compound **5h**. 58 mg, 13%, yellow oil. MS (ESI, pos. ion) *m*/*z*: 299.0 ([M + H]$^+$); ^{1}H NMR (400 MHz, $CDCl_3$): δ (ppm) 6.21 (d, *J* = 12.0 Hz, 2H), 3.88 (m, 2H), 3.77 (s, 3H), 3.44 (m, 1H), 2.93 (s, 6H), 2.83 (ABX, *J* = 17.2, 8.0, 9.7 Hz, 2H); ^{19}F NMR (376 MHz, $CDCl_3$): δ (ppm) −118.84 (s), −119.67 (s); ^{13}C NMR (151 MHz, $CDCl_3$): δ (ppm) 173.0, 172.7, 159.8 (dd, $^1J_{CF}$ = 246.9, $^3J_{CF}$ = 8.4 Hz), 151.2 (t, $^3J_{CF}$ = 13.1 Hz), 102.2 (t, $^3J_{CF}$ = 17.6 Hz), 95.4 (dd, $^2J_{CF}$ = 24.0, $^3J_{CF}$ = 3.7 Hz), 52.6, 51.3, 40.3, 37.2, 33.4; HRMS (ESI-TOF) *m*/*z*: [M + H]$^+$ calcd for $C_{14}H_{17}F_2N_2O_3$ 299.1207, found: 299.1218.

Compound **6i**: 85 mg, 61%, yellow oil. MS (ESI, pos. ion) *m*/*z*: 274.2 ([M + H]$^+$); ^{1}H NMR (400 MHz, $CDCl_3$): δ (ppm) 6.74 (p, *J* = 3.2 Hz, 2H), 3.97–3.84 (m, 2H), 3.76 (s, 3H), 3.46 (dt, *J* = 16.1, 8.0 Hz, 1H), 2.83 (ABX, *J* = 17.3, 7.7, 9.6 Hz, 2H); ^{19}F NMR (376 MHz, $CDCl_3$): δ (ppm) −107.20 (t, *J* = 6.0 Hz), −113.92 (s), −114.72 (s); ^{13}C NMR (151 MHz, $CDCl_3$): δ (ppm) 172.6, 172.3, 162.7 (t, $^3J_{CF}$ = 14.8 Hz), 161.0 (t, $^3J_{CF}$ = 14.8 Hz), 159.2 (ddd, $^1J_{CF}$ = 254.0, $^3J_{CF}$ = 15.3, 7.4 Hz), 111.5 (td, $^3J_{CF}$ = 16.6, 5.1 Hz), 101.2 (t, $^2J_{CF}$ = 25.1 Hz), 52.7, 50.7, 37.2, 33.2; HRMS (ESI-TOF) *m*/*z*: [M + H]$^+$ calcd for $C_{12}H_{11}F_3NO_3$ 274.0691, found: 274.0647.

Compound **6j**: 132 mg, 59%, yellow oil. MS (ESI, pos. ion) *m*/*z*: 290.1 ([M + H]$^+$); ^{1}H NMR (400 MHz, $CDCl_3$): δ (ppm) 6.97 (d, *J* = 8.1 Hz, 2H), 3.88 (p, *J* = 9.5 Hz, 2H), 3.71 (s, 3H), 3.43 (dt, *J* = 16.0, 7.8 Hz, 1H), 2.79 (ABX, *J* = 17.4, 7.6, 9.6 Hz, 2H); ^{19}F NMR (376 MHz, $CDCl_3$): δ (ppm) −114.90 (s), −115.58 (s); ^{13}C NMR (151 MHz, $CDCl_3$): δ (ppm) 172.4, 172.1, 158.6 (dd, $^1J_{CF}$ = 255.7, $^3J_{CF}$ = 6.3 Hz), 134.4 (t, $^3J_{CF}$ = 12.7 Hz), 113.8 (t, $^3J_{CF}$ = 16.5 Hz), 113.3 (dd, $^2J_{CF}$ = 23.1, $^3J_{CF}$ = 1.5 Hz), 52.6, 50.5, 37.1, 33.0; HRMS (ESI-TOF) *m*/*z*: [M + H]$^+$ calcd for $C_{12}H_{11}ClF_2NO_3$ 290.0396, found: 290.0349.

Compound **6k**: 112 mg, 42%, yellow oil. MS (ESI, pos. ion) *m*/*z*: 334.0 ([M + H]$^+$); ^{1}H NMR (400 MHz, $CDCl_3$): δ (ppm) 7.18 (d, *J* = 7.8 Hz, 2H), 4.00–3.87 (m, 2H), 3.78 (s, 3H), 3.53–3.40 (m, 1H), 2.85 (ABX, *J* = 17.4, 7.7, 9.6 Hz, 2H); ^{19}F NMR (376 MHz, $CDCl_3$): δ (ppm) −114.94 (s), −115.72 (s); ^{13}C NMR (151 MHz, $CDCl_3$): δ (ppm) 172.6, 172.1, 158.8 (dd, $^1J_{CF}$ = 256.8, $^3J_{CF}$ = 6.0 Hz), 121.5 (t, $^3J_{CF}$ = 11.8 Hz), 116.4 (d, $^2J_{CF}$ = 22.9 Hz), 114.4 (t, $^3J_{CF}$ = 16.2 Hz), 52.8, 50.7, 37.4, 33.3; HRMS (ESI-TOF) *m*/*z*: [M + H]$^+$ calcd for $C_{12}H_{11}BrF_2NO_3$ 333.9890, found: 333.9885.

Compound **6l**: 65 mg, 37%, yellow oil. MS (ESI, pos. ion) *m*/*z*: 382.0 ([M + H]$^+$); ^{1}H NMR (400 MHz, $CDCl_3$): δ (ppm) 7.36 (d, *J* = 7.6 Hz, 2H), 4.01–3.84 (m, 2H), 3.78 (s, 3H), 3.53–3.39 (m, 1H), 2.84 (ABX, *J* = 17.4, 7.7, 9.6 Hz, 2H); ^{19}F NMR (376 MHz, $CDCl_3$): δ (ppm) −115.44 (s), −116.20 (s); ^{13}C NMR (151 MHz, $CDCl_3$): δ (ppm) 172.6, 172.1, 158.5 (dd, $^1J_{CF}$ = 258.2, $^3J_{CF}$ = 5.4 Hz), 122.1 (d, $^2J_{CF}$ = 22.2 Hz), 115.2 (t, $^3J_{CF}$ = 16.3 Hz), 91.0 (t, $^3J_{CF}$ = 10.0 Hz), 52.8, 50.6, 37.4, 33.3; HRMS (ESI-TOF) *m*/*z*: [M + H]$^+$ calcd for $C_{12}H_{11}F_2INO_3$ 381.9752, found: 381.9997.

Compound **6o**: 154 mg, 73%, yellow oil. MS (ESI, pos. ion) *m*/*z*: 300.1 ([M + H]$^+$); ^{1}H NMR (400 MHz, $CDCl_3$): δ (ppm) 6.50 (d, *J* = 10.1 Hz, 2H), 3.98 (q, *J* = 7.0 Hz, 2H), 3.95–3.83 (m, 2H), 3.77 (s, 3H), 3.52–3.38 (m, 1H), 2.84 (ABX, *J* = 17.2, 7.8, 9.6 Hz, 2H), 1.40 (t, *J* = 7.0 Hz, 3H); ^{19}F NMR (376 MHz, $CDCl_3$): δ (ppm) −117.02 (s), −117.89 (s); ^{13}C NMR (151 MHz, $CDCl_3$): δ (ppm) 172.8, 172.5, 159.5 (dd, $^1J_{CF}$ = 250.2, $^3J_{CF}$ = 8.0 Hz), 159.8 (t, $^3J_{CF}$ = 13.3 Hz), 107.2 (t, $^3J_{CF}$ = 17.1 Hz), 99.1 (dd, $^2J_{CF}$ = 23.5, $^3J_{CF}$ = 2.9 Hz), 64.6, 52.7, 51.1, 37.2, 33.4, 14.6; HRMS (ESI-TOF) *m*/*z*: [M + H]$^+$ calcd for $C_{14}H_{16}F_2NO_4$ 300.1047, found: 300.1048.

Compound **6u**: 65 mg, 33%, yellow oil. MS (ESI, pos. ion) *m*/*z*: 281.0 ([M + H]$^+$); ^{1}H NMR (400 MHz, $CDCl_3$): δ (ppm) 7.30 (d, *J* = 7.8 Hz, 2H), 4.06–3.89 (m, 2H), 3.77 (s, 3H), 3.55–3.41 (m, 1H), 2.85 (ABX, *J* = 17.5, 7.5, 9.5 Hz, 2H); ^{19}F NMR (376 MHz, $CDCl_3$): δ (ppm) −111.95 (s), −112.30 (s); ^{13}C NMR (151 MHz, $CDCl_3$): δ (ppm) 172.3, 171.8, 158.7 (dd, $^1J_{CF}$ = 257.0, $^3J_{CF}$ = 5.7 Hz), 120.3 (t, $^3J_{CF}$ = 16.0 Hz), 116.6 (dd, $^2J_{CF}$ = 23.9, $^3J_{CF}$ = 3.8 Hz), 116.2 (t, $^3J_{CF}$ = 3.2 Hz), 112.6 (t, $^3J_{CF}$ = 11.6 Hz), 52.8, 50.5, 37.5, 33.2; HRMS (ESI-TOF) *m*/*z*: [M + H]$^+$ calcd for $C_{13}H_{11}F_2N_2O_3$ 281.0738, found: 281.0728.

© 2022 The Author(s). Published by the Royal Society of Chemistry

Open Access Article. Published on 09 November 2022. Downloaded on 2/10/2026 6:58:20 PM.
This article is licensed under a Creative Commons Attribution-NonCommercial 3.0 Unported Licence.

Compound **6p**: To a solution of compound **6l** (260 mg, 0.68 mmol), tributyl(vinyl)stannane (221 mg, 0.70 mmol) and chlorolithium (95 mg, 2.25 mmol) in DMF (5 mL) was added $PdCl_2(PPh_3)_2$ (62 mg, 0.1 mmol) and charged with N_2. The reaction mixture was heated to 80 °C and stirred overnight, then concentrated *in vacuo*. The residue was purified by a flash column chromatography (EtOAc/PE (v/v) = 1/10 to 1/5) to give compound **6p** (140 mg, 73%) as colorless oil; MS (ESI, pos. ion) *m*/*z*: 282.0 ($[M + H]^+$); ^{1}H NMR (400 MHz, $CDCl_3$): δ (ppm) 7.00 (d, J = 9.5 Hz, 2H), 6.60 (dd, J = 17.5, 10.8 Hz, 1H), 5.75 (d, J = 17.5 Hz, 1H), 5.38 (d, J = 10.8 Hz, 1H), 4.03–3.86 (m, 2H), 3.78 (s, 3H), 3.54–3.41 (m, 1H), 2.86 (ABX, J = 17.3, 7.8, 9.6 Hz, 2H); ^{19}F NMR (376 MHz, $CDCl_3$): δ (ppm) −117.42 (s), −118.16 (s); ^{13}C NMR (151 MHz, $CDCl_3$): δ (ppm) 172.7, 172.2, 158.9 (dd, $^1J_{CF}$ = 252.2, $^3J_{CF}$ = 6.0 Hz), 139.7 (t, $^3J_{CF}$ = 9.4 Hz), 134.6, 117.4, 113.8 (t, $^3J_{CF}$ = 16.9 Hz), 109.8 (d, $^2J_{CF}$ = 20.7 Hz), 52.7, 50.9, 37.4, 33.4; HRMS (ESI-TOF) *m*/*z*: $[M + H]^+$ calcd for $C_{14}H_{14}F_2NO_3$ 282.0942, found: 282.0931.

Compound **6q**: the method as compound **6p**. 337 mg, 81%, colorless oil. MS (ESI, pos. ion) *m*/*z*: 296.1 ($[M + H]^+$); ^{1}H NMR (400 MHz, $CDCl_3$): δ (ppm) 6.91 (d, J = 9.8 Hz, 2H), 6.35–6.18 (m, 2H), 4.01–3.85 (m, 2H), 3.78 (s, 3H), 3.54–3.40 (m, 1H), 2.85 (ABX, J = 17.3, 7.8, 9.6 Hz, 2H), 1.87 (d, J = 5.0 Hz, 3H); ^{19}F NMR (376 MHz, $CDCl_3$): δ (ppm) −117.98 (s), −118.75 (s); ^{13}C NMR (151 MHz, $CDCl_3$): δ (ppm) 172.7, 172.3, 158.9 (dd, $^1J_{CF}$ = 251.5, $^3J_{CF}$ = 6.0 Hz), 140.2 (t, $^3J_{CF}$ = 9.7 Hz), 129.7, 128.9, 112.7 (t, $^3J_{CF}$ = 16.8 Hz), 109.3 (d, $^2J_{CF}$ = 20.4 Hz), 52.7, 50.9, 37.4, 33.4, 18.5; HRMS (ESI-TOF) *m*/*z*: $[M + H]^+$ calcd for $C_{15}H_{16}F_2NO_3$ 296.1098, found: 296.1099.

Compound **6m**: the method as compound **5f**. 82 mg, 91%, colorless oil. MS (ESI, pos. ion) *m*/*z*: 284.1 ($[M + H]^+$); ^{1}H NMR (400 MHz, $CDCl_3$): δ (ppm) 6.81 (d, J = 9.3 Hz, 2H), 4.00–3.85 (m, 2H), 3.77 (s, 3H), 3.47 (dt, J = 16.4, 8.1 Hz, 1H), 2.85 (ABX, J = 17.2, 7.8, 9.6 Hz, 2H), 2.63 (q, J = 7.6 Hz, 2H), 1.22 (t, J = 7.6 Hz, 3H); ^{19}F NMR (376 MHz, $CDCl_3$): δ (ppm) −118.28 (s), −119.07 (s); ^{13}C NMR (101 MHz, $CDCl_3$): δ (ppm) 172.7, 172.3, 158.7 (dd, $^1J_{CF}$ = 252.0, $^3J_{CF}$ = 5.8 Hz), 147.0 (t, $^3J_{CF}$ = 8.8 Hz), 112.0 (t, $^3J_{CF}$ = 16.7 Hz), 111.6 (d, $^3J_{CF}$ = 19.8 Hz), 52.6, 50.9, 37.3, 33.4, 28.8, 14.9; HRMS (ESI-TOF) *m*/*z*: $[M + H]^+$ calcd for $C_{14}H_{16}F_2NO_3$ 284.1098, found: 284.1092.

Compound **6n**: the method as compound **5f**. 77 mg, 84%, colorless oil. MS (ESI, pos. ion) *m*/*z*: 298.1 ($[M + H]^+$); ^{1}H NMR (400 MHz, $CDCl_3$): δ (ppm) 6.78 (d, J = 9.4 Hz, 2H), 4.01–3.84 (m, 2H), 3.76 (s, 3H), 3.52–3.39 (m, 1H), 2.84 (ABX, J = 17.2, 7.8, 9.6 Hz, 2H), 2.55 (t, J = 7.6 Hz, 2H), 1.68–1.54 (m, 2H), 0.93 (t, J = 7.3 Hz, 3H); ^{19}F NMR (376 MHz, $CDCl_3$): δ (ppm) −118.39 (s), −119.16 (s); ^{13}C NMR (151 MHz, $CDCl_3$): δ (ppm) 172.7, 172.3, 158.6 (dd, $^1J_{CF}$ = 252.0, $^3J_{CF}$ = 5.6 Hz), 145.5 (t, $^3J_{CF}$ = 8.8 Hz), 112.0 (t, $^3J_{CF}$ = 17.0 Hz), 52.7, 50.9, 37.8, 37.3, 33.4, 24.0, 13.7; HRMS (ESI-TOF) *m*/*z*: $[M + H]^+$ calcd for $C_{15}H_{18}F_2NO_3$ 298.1255, found: 298.1252.

Compound **6r**: to a solution of compound **6l** (383 mg, 1.00 mmol), phenylboronic acid (247 mg, 2.03 mmol) and sodium carbonate (233 mg, 2.2 mmol) in 1,4-dioxane (2 mL) and water (2 mL) was added $Pd(dppf)Cl_2 \cdot CH_2Cl_2$ (165 mg, 0.20 mmol) and charged with N_2. The reaction mixture was heated to 100 °C and stirred overnight, then concentrated *in vacuo*. The residue was purified by a flash column chromatography (EtOAc/PE (v/v) = 1/10 to 1/1) to give compound **6r** (270 mg, 82%) as colorless oil; MS (ESI, pos. ion) *m*/*z*: 332.1 ($[M + H]^+$); ^{1}H NMR (400 MHz, $CDCl_3$): δ (ppm) 7.49 (d, J = 7.4 Hz, 2H), 7.40 (m, 3H), 7.18 (d, J = 9.7 Hz, 2H), 3.97 (p, J = 9.6 Hz, 2H), 3.76 (s, 3H), 3.55–3.42 (m, 1H), 2.86 (ABX, J = 17.4, 7.6, 9.6 Hz, 2H); ^{19}F NMR (376 MHz, $CDCl_3$): δ (ppm) −116.85 (s), −117.62 (s); ^{13}C NMR (151 MHz, $CDCl_3$): δ (ppm) 172.8, 172.7, 158.9 (dd, $^1J_{CF}$ = 252.4, $^3J_{CF}$ = 5.9 Hz), 143.4 (t, $^3J_{CF}$ = 9.6 Hz), 138.3, 129.2, 128.8, 127.0, 113.3 (t, $^3J_{CF}$ = 16.8 Hz), 110.8 (dd, $^2J_{CF}$ = 20.9, $^3J_{CF}$ = 2.7 Hz), 52.7, 51.0, 37.3, 33.4; HRMS (ESI-TOF) *m*/*z*: $[M + H]^+$ calcd for $C_{18}H_{16}F_2NO_3$ 332.1098, found: 332.1089.

Compound **6s**: to a solution of compound **6l** (439 mg, 1.15 mmol), 1,2-bis(diphenylphosphino)ethane (50 mg, 0.12 mmol), diacetylpalladium (14 mg, 0.07 mmol) and formyloxysodium (165 mg, 2.43 mmol) in DMSO (4 mL) was added 2,2-dimethylpropanenitrile (1.5 mL) and charged with N_2. The reaction mixture was heated to 120 °C and stirred overnight, then concentrated *in vacuo*. The residue was purified by a flash column chromatography (EtOAc/PE (v/v) = 1/10 to 1/1) to give compound **6s** (160 mg, 49%) as colorless oil; MS (ESI, pos. ion) *m*/*z*: 284.1 ($[M + H]^+$); ^{1}H NMR (400 MHz, $CDCl_3$): δ (ppm) 9.92 (s, 1H), 7.51 (d, J = 8.2 Hz, 2H), 4.12–3.91 (m, 2H), 3.79 (s, 3H), 3.57–3.44 (m, 1H), 2.89 (ABX, J = 17.4, 7.6, 9.6 Hz, 2H); ^{19}F NMR (376 MHz, $CDCl_3$): δ (ppm) −113.13 (s), −113.72 (s); ^{13}C NMR (151 MHz, $CDCl_3$): δ (ppm) 188.8, 172.4, 171.9, 159.2 (dd, $^1J_{CF}$ = 256.7, $^3J_{CF}$ = 4.6 Hz), 136.7 (t, $^3J_{CF}$ = 7.2 Hz), 130.0 (d, $^3J_{CF}$ = 4.4 Hz), 120.6 (t, $^3J_{CF}$ = 16.5 Hz), 113.0 (d, $^2J_{CF}$ = 20.7 Hz), 52.8, 50.6, 37.5, 33.3; HRMS (ESI-TOF) *m*/*z*: $[M + H]^+$ calcd for $C_{13}H_{12}F_2NO_4$ 284.0734, found: 284.0750.

Compound **6t**: to a solution of compound **6l** (382 mg, 1.00 mmol), 1,3-bis(diphenylphosphino)propane (87 mg, 0.20 mmol), diacetylpalladium (27 mg, 0.14 mmol) and Na_2CO_3 (298 mg, 2.81 mmol) in *n*-butanol (3 mL) was added 1-vinyloxybutane (504 mg, 5.03 mmol) and charged with N_2. The reaction mixture was heated to 120 °C and stirred overnight, then concentrated *in vacuo*. The residue was purified by a flash column chromatography (EtOAc/PE (v/v) = 1/10 to 1/2) to give compound **6t** (122 mg, 41%) as colorless oil; MS (ESI, pos. ion) *m*/*z*: 298.4 ($[M + H]^+$); ^{1}H NMR (400 MHz, $CDCl_3$): δ (ppm) 7.56 (d, J = 8.8 Hz, 2H), 4.08–3.91 (m, 2H), 3.79 (s, 3H), 3.50 (dt, J = 16.0, 8.0 Hz, 1H), 2.89 (ABX, J = 17.4, 7.7, 9.5 Hz, 2H), 2.58 (s, 3H); ^{19}F NMR (376 MHz, $CDCl_3$): δ (ppm) −114.25, 114.86 (s); ^{13}C NMR (101 MHz, $CDCl_3$) δ 194.8, 172.5, 171.9, 158.8 (dd, $^1J_{CF}$ = 255.3, $^3J_{CF}$ = 5.2 Hz), 137.8 (t, $^3J_{CF}$ = 7.2 Hz), 130.1 (d, $^3J_{CF}$ = 3.4 Hz), 119.6–119.0 (m), 112.2 (d, $^3J_{CF}$ = 18.4 Hz), 52.8, 50.7, 37.5, 33.4, 26.6; HRMS (ESI-TOF) *m*/*z*: $[M + H]^+$ calcd for $C_{14}H_{14}F_2NO_4$ 298.0891, found: 298.0902.

Compound **6v**: a solution of compound **6f** (568 mg, 2.10 mmol) in formic acid (7 mL) was heated to reflux and stirred for 1 h. The reaction was quenched with saturated Na_2CO_3 solution (100 mL), then extracted with dichloromethane (100 mL × 3). The combined organic phases were washed with brine (100 mL), dried over anhydrous Na_2SO_4 and concentrated *in vacuo*. The residue was purified by a flash column chromatography (EtOAc/PE (v/v) = 1/10 to 3/1) to give compound **6v** (322 mg, 51%) as yellow oil; MS (ESI, pos. ion) *m*/

Open Access Article. Published on 09 November 2022. Downloaded on 2/10/2026 6:58:20 PM. This article is licensed under a Creative Commons Attribution-NonCommercial 3.0 Unported Licence.

z: 299.0 ($[M + H]^+$); ^{1}H NMR (400 MHz, $CDCl_3$): δ (ppm) 9.04 (s, 1H), 8.20 (s, 1H), 7.08 (d, J = 12.6 Hz, 2H), 3.99–3.83 (m, 2H), 3.78 (s, 3H), 3.55–3.43 (m, 1H), 2.89 (ABX, J = 17.4, 7.4, 9.7 Hz, 2H); ^{19}F NMR (376 MHz, $CDCl_3$): δ (ppm) −117.46 (s), −117.98 (s); ^{13}C NMR (101 MHz, $CDCl_3$): δ (ppm) ^{13}C NMR (101 MHz, $CDCl_3$) δ 173.8, 172.5, 159.6, 158.7 (dd, $^1J_{CF}$ = 250.3, $^3J_{CF}$ = 6.6 Hz), 139.1 (t, $^3J_{CF}$ = 13.4 Hz), 109.6 (t, $^3J_{CF}$ = 17.0 Hz), 103.9 (dd, $^2J_{CF}$ = 24.7, $^3J_{CF}$ = 3.0 Hz), 52.8, 51.4, 37.2, 33.5; HRMS (ESI-TOF) *m*/*z*: $[M + H]^+$ calcd for $C_{13}H_{13}F_2N_2O_4$ 299.0843, found: 299.0841.

Compound **6w**: to a solution of compound **6f** (139 mg, 0.51 mmol), acetic acid (163 mg, 2.72 mmol), and Et_3N (298 mg, 2.81 mmol) in CH_2Cl_2 (10 mL) was added HATU (383 mg, 1.01 mmol). The reaction mixture was heated to reflux and stirred overnight, then concentrated *in vacuo*. The residue was purified by a flash column chromatography (EtOAc/PE (v/v) = 1/10 to 1/0) to give compound **6w** (139 mg, 87%) as yellow oil; MS (ESI, pos. ion) *m*/*z*: 313.1 ($[M + H]^+$); ^{1}H NMR (400 MHz, $CDCl_3$): δ (ppm) 9.09 (s, 1H), 7.04 (d, J = 10.8 Hz, 2H), 3.96–3.84 (m, 2H), 3.78 (s, 3H), 3.55–3.43 (m, 1H), 2.91 (ABX, J = 17.4, 7.4, 9.7 Hz, 2H), 2.05 (s, 3H); ^{19}F NMR (376 MHz, $CDCl_3$): δ (ppm) −118.54 (s), −119.11 (s); ^{13}C NMR (151 MHz, $CDCl_3$): δ (ppm) ^{13}C NMR (101 MHz, $CDCl_3$) δ 174.0, 172.6, 169.4, 158.7 (dd, $^1J_{CF}$ = 249.3, $^3J_{CF}$ = 6.6 Hz), 140.4 (t, $^3J_{CF}$ = 13.4 Hz), 108.6 (t, $^3J_{CF}$ = 17.1 Hz), 103.3 (d, $^2J_{CF}$ = 25.8 Hz), 52.9, 51.6, 37.1, 33.6, 24.2; HRMS (ESI-TOF) *m*/*z*: $[M + H]^+$ calcd for $C_{14}H_{15}F_2N_2O_4$ 313.1000, found: 313.0999.

Conflicts of interest

There are no conflicts to declare.

Notes and references

1 (*a*) M. Inoue, Y. Sumii and N. Shibata, *ACS Omega*, 2020, **5**, 10633–10640; (*b*) Y. Zhou, J. Wang, Z. Gu, S. Wang, W. Zhu, J. L. Acena, V. A. Soloshonok, K. Izawa and H. Liu, *Chem. Rev.*, 2016, **116**, 422–518.

2 X. Li, K. Christopher and F. B. Matthew, *J. Fluorine Chem.*, 2017, **198**, 47–53.

3 D. Diana Gimenez, A. Aoife Phelan, C. D. Murphy and S. L. Cobb, *Beilstein J. Org. Chem.*, 2021, **17**, 293–318.

4 Z. Xu, C. Liu, S. Zhao, S. Chen and Y. Zhao, *Chem. Rev.*, 2019, **119**, 195–230.

5 (*a*) Y. Zhao and T. M. Swager, *J. Am. Chem. Soc.*, 2015, **137**, 3221–3224; (*b*) Y. Zhao, G. Markopoulos and T. M. Swager, *J. Am. Chem. Soc.*, 2014, **136**, 10683–10690.

6 M. Sun, W. Chen, T. Zhang, Z. Liu, J. Wei and N. Xi, *Tetrahedron*, 2020, **76**, 131679.

7 (*a*) B. Huang, L. Xu, N. Wang, J. Ying, Y. Zhao and S. Huang, *Anal. Chem.*, 2022, **94**, 1867–1873; (*b*) C. Dong, Z. Xu, L. Wen, S. He, J. Wu, Q.-H. Deng and Y. Zhao, *Anal. Chem.*, 2021, **93**, 2968–2973.

8 C. R. Buchholz and W. C. K. Pomerantz, *RSC Chem. Biol.*, 2021, **2**, 1312–1330.

9 J. X. Yu, R. R. Hallac, S. Chiguru and R. P. Mason, *Nucl. Magn. Reson. Spectrosc.*, 2013, **70**, 25–49.

10 K. Muller, C. Faeh and F. Diederich, *Science*, 2007, **317**, 1881–1886.

11 (*a*) C. Dalvit and A. Vulpetti, *Chem.–Eur. J.*, 2016, **22**, 7592–7601; (*b*) R. Taylor, *Acta Crystallogr, Sect. B: Struct. Sci., Cryst. Eng. Mater.*, 2017, **73**, 474–488.

12 (*a*) M. R. Bauer, R. N. Jones, M. G. J. Baud, R. Wilcken, F. M. Boeckler, A. R. Fersht, A. C. Joerger and J. Spencer, *ACS Chem. Bio.*, 2016, **11**, 2265–2274; (*b*) P. Li, J. M. Maier, E. C. Vik, C. J. B. Yehl, E. Dial, A. E. Rickher, M. D. Smith, P. J. Pellechia and K. D. Shimizu, *Angew. Chem.Int. Ed.*, 2017, **56**, 7209–7212.

13 (*a*) J. Shang, N. M. Gallagher, F. Bie, Q. Li, Y. Che, Y. Wang and H. Jiang, *J. Org. Chem.*, 2014, **79**, 5134–5144; (*b*) C. Dalvit, C. Invernizzi and A. Vulpetti, *Chem.–Eur. J.*, 2014, **20**, 11058–11068.

14 (*a*) M. D. Struble, J. Strull, K. Patel, M. A. Siegler and T. Lectka, *J. Org. Chem.*, 2014, **79**, 1–6; (*b*) M. D. Struble, M. T. Scerba, M. Siegler and T. Lectka, *Science*, 2013, **340**, 57–60; (*c*) C. R. Pitts, M. G. Holl and T. Lectka, *Angew. Chem., Int. Ed.*, 2018, **57**, 1924–1927; (*d*) M. G. Holl, C. R. Pitts and T. Lectka, *Angew. Chem.Int. Ed.*, 2018, **57**, 2–11.

15 N. Xi, X. H. Sun, M. X. Li, M. M. Sun, M. A. Xi, Z. P. Zhan, J. Yao, X. Bai, Y. J. Wu and M. Liao, *J. Org. Chem.*, 2018, **83**, 11586–11594.

16 N. Xi, M. Sun, Y. Lu and B. Bai, *Tetrahedron*, 2022, 132733.

17 M. J. Milewska, T. Bytner and T. Polonski, *Synthesis*, 1996, **12**, 1485–1488.

18 C. L. Lopez, S. Patterson, T. Blum, A. F. Straight, J. Toth, A. M. Z. Slawin, T. J. Mitchison, J. R. Sellers and N. J. Westwood, *Eur. J. Org. Chem.*, 2005, **2005**, 1736–1740.

19 F. K. Woolard, *US pat.*, US4909834, Richmond, Calif, 1990.

20 G. A. Grasa, P. Steven and S. P. Nolan, *Org. Lett.*, 2001, **3**, 119–122.

21 Y. Zhang, X. Jiang, J.-M. Wang, J.-L. Chen and Y.-M. Zhu, *RSC Adv.*, 2015, **5**, 17060–17063.

22 J. Mo, L. Xu and J. Xiao, *J. Am. Chem. Soc.*, 2005, **127**, 751–760.

23 Optimized structures and FMO orbitals were depicted with the GaussView 06 program.

24 P. Politze and J. S. Murray, *ChemPhysChem*, 2020, **21**, 579–588.

25 (*a*) A. Rodrigo Cormanich, R. Rittner, D. O, Hagan and M. Bühl, *J. Comput. Chem.*, 2016, **37**, 25–33; (*b*) K. J. Kamer, A. Choudhary and R. T. Raines, *J. Org. Chem.*, 2013, **78**, 2099–2103; (*c*) R. W. Newberry and R. T. Raines, *Acc. Chem. Res.*, 2017, **50**, 1838–1846.

26 D. J. Pascoe, K. B. Ling and S. L. Cockroft, *J. Am. Chem. Soc.*, 2017, **139**, 15160–15167.

27 N. Lu, R. M. Ley, C. E. Cotton, W.-C. Chung, J. S. Francisco and E. Negishi, *J. Phys. Chem. A*, 2013, **117**, 8256–8262.

28 S. Hanessian, O. M. Saavedra, M. A. Vilchis-Reyes, J. P. Maianti, H. Kanazawa, P. Dozzo, R. D. Matias, A. Serio and J. Kondo, *Chem. Sci.*, 2014, **5**, 4621–4632.

© 2022 The Author(s). Published by the Royal Society of Chemistry